GEOPHYSICAL STRUCTURE OF THE SOUTHERN ALPS OROGEN, SOUTH ISLAND, NEW ZEALAND.

F J Davey[1], D Eberhart-Phillips[2], M D Kohler[3], S Bannister[1], G Caldwell[1], S Henrys[1], M Scherwath[4], T Stern[5], and H van Avendonk[6]

[1]GNS Science, Gracefield, Lower Hutt, New Zealand, f.davey@gns.cri.nz
[2]GNS Science, Dunedin, New Zealand
[3]Center for Embedded Networked Sensing, University of California, Los Angeles, California, USA
[4]Leibniz-Institute of Marine Sciences, IFM-GEOMAR, Kiel, Germany
[5]School of Earth Sciences, Victoria University of Wellington, Wellington, New Zealand
[6]Institute of Geophysics, University of Texas, Austin, Texas, USA

ABSTRACT

The central part of the South Island of New Zealand is a product of the transpressive continental collision of the Pacific and Australian plates during the past 5 million years, prior to which the plate boundary was largely transcurrent for over 10 My. Subduction occurs at the north (west dipping) and south (east dipping) of South Island. The deformation is largely accommodated by the ramping up of the Pacific plate over the Australian plate and near-symmetric mantle shortening. The initial asymmetric crustal deformation may be the result of an initial difference in lithospheric strength or an inherited suture resulting from earlier plate motions. Delamination of the Pacific plate occurs resulting in the uplift and exposure of mid-crustal rocks at the plate boundary fault (Alpine fault) to form a foreland mountain chain. In addition, an asymmetric crustal root (additional 8 - 17 km) is formed, with an underlying mantle downwarp. The crustal root, which thickens southwards, comprises the delaminated lower crust and a thickened overlying middle crust. Lower crust is variable in thickness along the orogen, which may arise from convergence in and lower lithosphere extrusion along the orogen. Low velocity zones in the crust

occur adjacent to the plate boundary (Alpine fault) in the Australian and Pacific plates, where they are attributed to fracturing of the upper crust as a result of flexural bending for the Australian plate and to high pressure fluids in the crust derived from prograde metamorphism of the crustal rocks for the Pacific plate.

INTRODUCTION

The Pacific-Australian plate boundary crosses the length of the South Island of New Zealand (Figure 1), where it is dominantly a transpressive boundary linking the east-dipping subduction zone southwest of the South Island from west-dipping subduction east of the North Island. The South Island's existence is largely the result of the plate tectonic deformation of the region along the Pacific-Australian plate boundary since its inception during the mid-Cenozoic. Prior to this time, the land mass of the South Island was extremely low lying, with only a small proportion of the present landmass above sea level (Suggate et al., 1978, Balance, 1993). This was due to extension and thinning of the New Zealand micro-continent lithosphere during late Cretaceous extension, and erosion and subsidence (cooling) associated with the break-up of Gondwana and onset of seafloor spreading between New Zealand, Australia and Antarctica. About 45 Ma ago the Pacific-Australian plate boundary developed, extending from the rifted margin off southwest Campbell Plateau, through the axis of the present South Island and along the convergent margin off east and north North Island to the old Cretaceous convergent margin off east Australia (Sutherland 1999). Initially this plate margin was dominantly transtensional, but it developed mainly as a transcurrent boundary until, at about 5 Ma, a significant component of convergence commenced leading to the thickening of the lithosphere and the emergence of the South Island and Southern Alps in particular. The structure and development of this orogen and the adjacent region during this transpressive phase is the focus of this chapter.

We first review the range of geophysical data available for the South Island. These data are then used to define the main features of the three-dimensional structure of the orogen and provide the context for the detailed structure and development of the plate boundary zone as defined by the Alpine Fault. The chapter closely complements the previous chapter on the geological data base for the South Island, and uses those and other data to constrain its inferences. The conclusions of the

analysis give models that provide a baseline of the general features for continental transpressive plate boundaries as discussed in the latter part of this volume

GEOPHYSICAL CHARACTERISTICS OF THE SOUTH ISLAND COLLISIONAL OROGEN

i)Topography - The morphology of the South Island is well known with several digital elevation models available for the region (e.g. Etopo2, Land Information New Zealand). These models typically have resolutions of about 25 m. Figure 2 shows the morphology of the South Island based on a grid of 1000 m (sub-sampled from 25 m grid), adequate to bring out the dominant features of the morphology. In general terms, the morphology of the South Island consists of an axial mountain range, the Southern Alps, that is narrow and high in the central part but wider and lower to the north and south, and is flanked by coastal plains. The high central part of the Southern Alps has five main zones from west to east: i) a narrow coastal plain in the west, delineated at its eastern margin by a linear range front (Alpine Fault), ii) a steep, west to northwest dipping mountain front that rises to the main divide at over 3000 m elevation in its central part (see later), iii) an intermontane plateau at about 1000 m, iv) a steep slope on the eastern side of the mountains, leading into v) a broad, gently east-dipping coastal plain to the east coast (Figure 3b).

This simple two-dimensional morphology is modified in the north and south of the South Island (see also Cox and Sutherland, Chapter X, this volume). In the north, where splay faulting from the Alpine Fault to the east starts, the mountains become lower but wider, and extend to the east coast, thus terminating the northward extent of the eastern coastal plain (Figure 3a). Their maximum height is about 2500 m. The major splay faults coincide with distinct linear morphological features (Figure 2). Elevated morphology occurs west of the Alpine Fault trace in the northern region. In the south, the mountains are also lower, reaching maximum elevations of about 2500 m, and broader, covering most of the southern South Island (Figure 3c). The morphology of the region is less two-dimensional and reflects the grain of the geology that swings around from a NNE to a ESE trend. The Alpine Fault is a more subdued morphological feature, but it is still remarkably linear until it runs offshore at Milford Sound.

The region of maximum elevation of the Southern Alps coincides with the narrowest part of mountain belt where the highest uplift rates of up to 17 mm/y occur (Wellman, 1979; Adams, 1979). Erosion however, is taking place at about the same rate (Adams, 1980) so that the mountain ranges are in approximate dynamic equilibrium.

ii) Seismicity distribution - The major features of seismicity distribution in New Zealand have been known for some time. Hatherton (1980) reported on shallow seismicity for the period 1956-75. Subsequently Reyners (1989) reported on shallow and deep seismicity for the period 1964-87. The upgrade of the New Zealand National Seismograph Network (NZNSN) from analogue to digital instruments that took place between 1986 and the mid 1990s allowed a more comprehensive analysis to be made (Anderson and Webb, 1994). In Figure 4 we plot the distribution of seismicity up to 2002. The distribution of seismicity falls into three distinct zones that correspond in general to the plate tectonic context of South Island. In the north, the influence of the southern end of the Hikurangi subduction system is dominant. Deep seismicity in this region traces the subducting Pacific lithosphere along the eastern margin of northern South Island to depths of about 200 km (Figure 4c,d). The southwest termination of this deep seismicity is sharp and coincides closely with the region where the Wairau and Awatere Faults splay off eastwards from the Alpine Fault. Shallow seismicity (Figure 4b) is extensive and intense in this same region, and delineates some of the major faults including the eastern splay faults. Shallow seismicity is also intense west of the Alpine Fault in the northwest South Island, but no unequivocal causative faults have been identified. In the south of the South Island, the influence of the Puysegur-Fiordland subduction system dominates seismicity (Figure 4c,d). The intermediate-depth seismicity is restricted in extent defining a narrow, near-vertical zone up to 140 km deep under central-northern Fiordland that traces the subduction of the Australian plate north-eastwards from Puysegur Trench under southwest South Island. The detailed geometry of the subducted plate is controversial, as the part of the plate from the Puysegur trench to well under southern South Island is not well constrained by seismicity. This may partially arise from limited station coverage. The shallow seismicity in the region is concentrated above the deep seismicity, and presumably relates to the subduction process.

The region between the two subduction zones is nearly devoid of earthquakes below 25-km depth (Figure 4c,d), but detailed studies of parts of the region (e.g. Reyners, 1987, 1988) show abundant shallow seismicity and a low level of deeper seismicity. A major improvement in the knowledge of seismicity in the South Island, particularly under the Southern Alps, has resulted from the Southern Alps Passive Seismic Experiment (SAPSE, Anderson et al., 1997), where an array of 26 broadband and 14 short-period recording seismographs was deployed over the South Island, concentrated on the central Southern Alps for up to 12 months. The array recorded 5491 earthquakes and most of the shots of the active source seismic shooting of SIGHT (Davey et al., 1998). These data have allowed much more accurate seismicity locations (Figure 5) with depth errors < 3 km, as well as the production of a 3D tomographic model of P and S-wave velocity for the South Island (see next section and Figure 6) (Eberhart-Phillips and Bannister, 2002).

A major feature of the crustal seismicity distribution is its restriction to depths of less than 12 ± 2 km indicating the depth of brittle crust under the Southern Alps (Leitner et al., 2001). The maximum depth decreases to about 8 km under the region of maximum uplift in the central Southern Alps indicating localised elevated temperatures east of the Alpine Fault. The rate of seismicity is subdued in a similar region about 10 - 20 km southeast of the Alpine Fault. Distributed seismicity is observed throughout a roughly 80-km wide region southeast of the Alpine fault, with the greatest moment release in the vicinity of the Alpine Fault. The Southern Alps seismicity does not cluster along specific faults, indicating that a wide range of structures are producing slip. This was borne out in the Mw 6.7 1994 Arthur's Pass earthquake sequence (Figure 5) which activated a broad zone of seismicity with varied focal mechanisms, following the primary reverse faulting event (Abercrombie et al., 2000). Several tens of intermediate-depth earthquakes (30-97 km) have been recorded in central South Island (Reyners, 1987; Kohler and Eberhart-Phillips, 2003) some of which align on a zone dipping at about 18° generally west to northwest, down to about 60 km depth (Reyners, 1987, 2005). The earthquakes are not associated with crustal subduction but all lie within or on the margins of thickened crust or uppermost mantle seismic high-velocity anomalies (Kohler and Eberhart-Phillips, 2003). The earthquakes are generally small ($M_L \leq 4.0$) but Reyners (2005) infers a subcrustal depth (50 km) for the 1943 Lake Hawea M_W 5.9 earthquake.

iii*) 3D tomography, earthquake travel-time and receiver function studies* - Recordings of earthquakes and shots from the active source seismic experiment (SIGHT) were used for the derivation of 3D models of P-wave velocity and Vp/Vs ratios, constrained for the deeper part of the models by the gravity data coverage of the region (Eberhart-Phillips and Bannister, 2002). The models (Figure 6), accurate to 0.2 km/s in P-wave velocity, were derived using nodes with 8-40 km spacing horizontally and 3-10 km spacing vertically, with velocities allowed to vary smoothly between nodes and hypocentral parameters included in the inversion. The models show a broad downwarp of the 7.5 km/s velocity contour (indicative of Moho) to depths of about 35 km under the central Southern Alps that shallows towards the coast. The deepest part trends to the east away from the highest part the Southern Alps following the axis of the gravity low (see later). A low-velocity layer occurs in the middle crust under the south-eastern part of the Southern Alps (Figure 6b, see also Reyners and Cowan, 1993; Kleffmann, 1999). Low-velocity zones are imaged along the Alpine Fault, and are southeast-dipping in the central oblique-slip region and vertical in the southern strike-slip region (Figure 6). Given the sparse data and coarse grid, it is not possible to fully define the subsurface fault zone. There are clear differences in the low-velocity zone between the central and southern sections, and the character at 14-km depth compared to 6-km depth (Figure 6a-b). At 14-km depth, the low-velocity zone appears as a distinct feature trending to the southeast away from the Alpine Fault, such that it does not join up with the southern Alpine Fault low-velocity zone Figure 6b). The variation in the thickness of the incoming Pacific plate is shown in the 30-km depth velocity slice (Figure 6c). The crust is thinner in the Canterbury (east-central South Island) region, and thickens by 5-10 km towards the southeast. The shape of the crustal root is shown by the large low-velocity region (Figure 6c). This extends well south of the oblique-slip fault section, with the most pronounced low velocity occurring 80 km south of Mt. Cook. The crustal root is also seen in the cross-sections (Figure 6d-g), where both vertical and dipping lines are shown for the Alpine fault, since the true variation of fault dip with depth is not known.

The tomographic model to the north (Eberhart-Phillips and Reyners, 1997) shows a relatively narrow velocity low throughout the crust associated with the Awatere Fault, a major splay fault of eastern South Island (northern white line, Figure 6a-b). In cross-section, the subducted slab is shown in both seismicity and velocity, with relatively low velocities between 40 and 100 km depth, reflecting the continental

nature of the subducted crust in this region (Figure 7). Strong P-wave anisotropy of up to 12% is found in the brittle crust in the region of the Awatere and Wairau Faults (Eberhart-Phillips and Henderson, 2004) and is aligned with faults (Figure 7). Different anisotropic azimuths are found in the more ductile region below 20-km depth in a zone of progressive coupling and partial subduction. They are more aligned with the relative plate motion and associated with crustal thickening (Fig. 6c). A detailed receiver function study along a profile across the Wairau Fault to the Clarence Fault (Wilson et al., 2004) inferred a southeast (along profile) dipping Moho (24 km deep north of the Wairau Fault to 34 km just south of the fault) under the region with pervasive anisotropy of unspecified orientation in the middle crust (15 -20 km) of the region. In the Fiordland subduction region in the south, tomographic velocity models (Eberhart-Phillips and Reyners, 2001) show high-velocity Pacific mantle below 80-km depth, which impinges on the subducted Australian slab and causes it to bend to near vertical (Figure 8).

Delays in teleseismic P-wave arrivals from distant earthquakes, detected by the detailed receiver arrays (about 80 seismographs each) along the two main transects of the SIGHT project, compared to a standard earth model have been used to define a high-velocity anomaly in the upper mantle under the crustal root (Stern et al., 2000). The delays across the array show a major advance (reduction in delay) across the South Island (see also Stern et al., Chapter NN this volume). The relative delays were modeled by correcting for the crustal velocity model derived from the active source experiment and assigning the residual delays to a broad vertical positive velocity anomaly in the upper mantle constrained by ray tracing. The preferred model for the velocity anomaly (maximum 7% wrt 8.1 km/s) is centred below the crustal root and is about 80 km wide, extending from 60 to 170 km in depth (dashed contours in Figure 9). The high density of seismographs along each transect and detailed ray tracing allowed Stern et al. (2000) to closely constrain the geometry and magnitude limits of the anomalous body in the upper mantle. They show that at least its western margin is within 15° of vertical. This model gives a local residual delay that Stern et al. (2000) assign to a low-velocity crust within the hanging wall of the Alpine Fault.

A three-dimensional uppermost mantle seismic velocity model below South Island has also been derived by teleseismic P-wave travel-time inversion using waveform data from the SAPSE experiment and the New Zealand National Seismograph Network (Kohler and Eberhart-Phillips, 2002). The velocity images

show a near-vertical, northwest dipping, high-velocity (2-4% relative to regionally average uppermost mantle velocities - 8.1 km/s) structure in the uppermost mantle (gray scale contours in Figure 9) that also directly underlies thickened crust along the NNE-SSW axis of the Southern Alps (east of the Alpine Fault) (Figure 10). It extends from about 40 km to 200 km in depth from the northern to the southern end of South Island. The seismic anomaly varies from 60 to 100 km in width. The narrowest portion corresponds to the narrowest region of crustal deformation in central and northern South Island, and the widest portion corresponds to the wider plate boundary deformation zone in Otago (Figure 10). The velocity anomaly does not appear to increase its dip with depth like a subducted oceanic lithospheric slab and its geometry can be visualized as a long sheet descending into the mantle. The anomaly is broadly similar to that derived by forward modeling of teleseismic P-wave delays noted earlier (Figure 10) but is less well constrained in dip and magnitude due to data distribution and smoothing involved in the tomographic inversion. Other tests indicated a partial (40%) recovery of anomaly amplitude that is best at shallower depths, and a northwest dip bias of about 10° for a vertical body.

The high upper mantle velocities obtained by Kohler and Eberhart-Phillips (2002) extend from the 100-km thick sheet in northwest Nelson to southern South Island. In the north, the high-velocity anomaly (3-5%) corresponds to the descending slab of the Hikurangi subduction zone, with a depth extent corresponding to the deepest seismicity. The anomaly indicates a gradual change from a slab environment associated with deep seismicity in the oceanic lithosphere to continental lithospheric collision conditions which are characterized by no deep seismicity. The images suggest that continental mantle lithospheric deformation takes over where subduction stops, but they do not provide evidence for a sharp oceanic lithospheric slab edge where the deep seismicity ends. In the south, the high-velocity structure at 100 km depth under eastern Fiordland is continuous with the Southern Alps high-velocity anomaly but extends deeper, to at least 220 km. Neither the teleseismic nor local earthquake studies of Fiordland find high velocities associated with the subducted Australian plate. It is relatively young (20-40 ma) and may be thinner, warmer, and less dense than older slabs (Kohler and Eberhart-Phillips, 2002).

Regional earthquake data have been used for Common Mid-Point (CMP) stacking of arrivals from local earthquakes recorded by the SIGHT transect recorders. They give an estimate of crustal thickness for South Island, indicating that the

Southern Alps crustal root thins and narrows north of the SIGHT transects (Wilson and Eberhart-Phillips, 1998). Aftershocks of Fiordland earthquakes observed on a profile along the Southern Alps indicate high Pn velocities (8.6 ± 0.1 km/s) and a crustal thickness increasing southwards to about 49 ± 6 km under southern South Island (Bourguiguon et al., Chapter X, this volume).

Teleseismic data have also been used for the calculation of shear-wave splitting using SKS phases. The results demonstrate strong anisotropy of the upper mantle under South Island where the fast component is NNE oriented over most of the South Island with a possible change to a more north orientation over the southern half of the island (Klosko et al., 1999, see also Savage et al., Chapter XX, this volume).

iv) *Wide angle active source/ velocity models* - Early active source seismic refraction and wide-angle measurements in the South Island have provided preliminary velocity models across central South Island (Smith et al., 1995), for the Lake Tekapo area (Kleffmann et al., 1998) and for the Fiordland area (Davey and Broadbent, 1980). The latter showed lower crustal velocities of about 7.3 km/s within 3 km of the surface associated with the large positive gravity anomaly in Fiordland. The results of the SIGHT project have superseded those of the former two projects. The SIGHT project recorded active source seismic measurements along two major transects (Transect 1 - T1 and Transect 2 - T2) across the South Island, and two main tie lines (Transect 3 - T3, and 3W) parallel to the coast (Fig 11, Davey et al., 1998; Stern at al., 1997). Measurements were made along the two main transects using explosive charges on land recorded by an array of 400 recorders placed on each transect across the South Island. These were supplemented by recording of offshore shots (airgun at 50 m spacing) by arrays of about 200 recorders on each line across the island and 17 ocean bottom seismographs offshore along each transect. Offshore vertical incidence reflection data constrained the sedimentary section along the offshore part of the transects. Seismic velocities along the northern transect, T1, were modelled (Figure 12a) by a tomographic inversion code (Van Avendonk et al., 2004) using dense parameterization that is adjusted to give the smoothest model with minimum residuals. T2 (Scherwath et al., 2003) and tie lines T3 off the east coast (Godfrey et al., 2001) and Line 3w of the west coast (Melhuish et al., 2004) have been modelled using the forward modelling and inversion code of Zelt and Smith (1992). This method uses sparse parameterization and minimum perturbation from the starting

model to minimise residuals. The different modelling techniques give rise to differences in the derived models (such as the broader crustal root in T1). The velocity models are shown in Figs 12b - d respectively. Ray coverage was good for most of T1 and T2 over the plate boundary. The deeper part of the crustal root is not well constrained due to poorer ray coverage.

The two main transects that cross the plate boundary have a number of features in common: similar crustal velocity structures under the coastal regions and further offshore, a low-velocity region around the Alpine Fault (plate boundary), and a thickened crustal section under the Southern Alps (although T2 was about 5 km thicker than T1, indicating changes along strike). T2 defined a low-velocity upper-mid crustal zone west of the west coast that has been attributed to flexural stress in the region (Scherwath et al., 2003). A low-velocity lower-mid crust in the Pacific Plate was detected on T2, similar to that detected on the passive seismic tomography models noted above. Upper mantle velocities on both T1 and T2 are generally above 8 km/s, however, a zone of reduced (7.6-7.7 km/s) uppermost mantle velocities exist around the plate boundary, extending to about 100 km offshore in the west. It's eastern limit is poorly resolved due to reduced data coverage below the crustal root.

The tie lines 3w and T3 (Figures 11 and 12) were designed to image the velocity structure of the South Island crust away from the region of present deformation and thus provide a crustal velocity model of the lithosphere that probably entered the deformation zone. Line 3w resulted in a fairly simple velocity model of thin crust with a well-defined reflective lower crust. The uppermost mantle velocities are high (8.5 km/s) at the southern end. Tie line T3 along the east coast of South Island has a fairly simple crustal model where it crosses the main transects T1 and T2, showing a thick upper crust and very thin lower crust. The uppermost mantle velocities for the intersecting east coast transects are all similar (8.1 - 8.3 km/s). The velocity model for T3 becomes more complex to the south probably resulting from the past deformation of multiple accreted terranes (Mortimer et al., 2002). There are significant changes in crustal thickness and a distinct localised low-velocity lower crust and uppermost mantle near Dunedin that was interpreted as remnant hot rock related to the Miocene Dunedin volcano. The crustal sections for all four transects agree to within 0.1-0.2 km/s and 1 km in depth where they cross.

To investigate crustal anisotropy in the vicinity of the Alpine Fault, Pulford et al., (2003) modelled SmS phases from transect T1 data for shear-wave splitting. A

maximum time difference of 0.08 s was measured indicating little or no anisotropy above 15 km for the direction of ray paths. However, significant upper mantle anisotropy occurs. The uppermost mantle P-wave velocities on line 3w are high (8.2 - 8.5 km/s) in contrast to velocities of about 7.6 - 7.8 km/s on the cross transects T1 and T2, implying significant uppermost mantle anisotropy (11±5% for T1-3w) in this region (Scherwath et al., 2002). The uppermost mantle velocities for the intersecting east coast transects are all similar, with velocities of 8.1 - 8.3 km/s for the intersections of T3 with T1 and T2 (Godfrey et al., 2001; Scherwath et al., 2003; Van Avendonk et al., 2004) implying little or no upper mantle anisotropy off the east coast.

v) MCS/CDP images - Crustal near-vertical incidence seismic reflection data (CDP) are limited to the coastal region of the South Island and along the main transects of the SIGHT project. In 1996, marine MCS reflection data were recorded to 16 s twt in association with the shots for the off-onshore experiments (Greenroyd et al., 2003; Mortimer et al., 2002; Godfrey et al., 2001; Melhuish et al., 2004; Davey, 2005). In 1998 CDP data were recorded overland along the central part of T2 and the west coast part of T1 (Henrys et al 1998). Extensive industry data exist for the east coast of the South Island (Field et al., 1989) and to a lesser extent for the West Coast (Nathan et al., 1986). They are useful for linking the SIGHT images to geological control at petroleum wells, but are limited in depth mainly to basement.

Interpreted Moho is well-recorded on all SIGHT96 reflection data, apart from the data corresponding to the far offshore (> 100 km from the coast) of the two trans-South Island transects (T1 and T2). Off the West Coast, the seismic images typically show a distinct base to the lower crustal reflectivity at about 9 s twt that is interpreted to be the Moho and corresponds very closely to refraction Moho. Above this is a highly reflective lower crust that is about 2 s twt thick and corresponds closely to a seismic refraction lower crust with velocities of 6.5 - 7.0 km/s, a relatively acoustically transparent upper crust with a consistent velocity of about 5.9 to 6.1 km/s, and a sedimentary section of variable thickness and character. Uppermost mantle dipping reflector packages have been imaged on the MCS data and are inferred to show old lithospheric convergent structures (Melhuish et al., 2004). Dipping mantle reflectors have been recorded on the wide angle data at apparent depths (ranges) of up to 100 km, but no precise locations have been derived.

The images off the east coast of South Island are more variable. Moho varies in character from a single reflector to the base of a highly reflective zone (Mortimer et al., 2002) and its depth varies strikingly from about 7.5 s twt to 11 s twt off southeast South Island (Figure 13). Off central South Island (Canterbury) the reflective lower crust is either thin or non-existent, corresponding in general to the wide-angle refraction results. It is overlain by an upper crust showing sparse, subdued and gently dipping reflectors that conform with the metamorphic grade of the greywackes and schists forming the crust in the south. The sedimentary section in this region is thick. Further south, the sediments thin and the crustal section becomes more complex (Mortimer et al., 2002) with a conspicuous, highly reflective lower crust of restricted lateral extent near Dunedin that is coincident with low lower crustal and upper mantle seismic velocities (Godfrey et al., 2001).

Off the southern part of the South Island, the seismic reflection images are complex. Moho is generally well-imaged at the base of a reflective lower crust with variable thickness. Dipping uppermost mantle events cross and displace the Moho, and are inferred to be major faults and paleosutures (Sutherland and Melhuish, 2000; Davey, 2005). The crustal sections consist of a reflective lower crust with a generally transparent upper crust overlain by a sedimentary section of variable thickness (Melhuish et al., 1999; Sutherland and Melhuish, 2000; Davey, 2005). In the southwest off Fiordland, seismic data show only the sedimentary section, and crustal reflectivity is poor (Wood et al., 2000). The seismic data image accretionary sediment packages along the highly obliquely convergent Fiordland margin (Barnes et al., 2005). A continental-oceanic plate boundary is inferred under the deep water of the upper continental rise (Wood et al., 2000).

The coverage of seismic reflection data on land in the South Island is limited. Surveys for petroleum or groundwater exploration have been undertaken for the main sedimentary basins of West Coast, Canterbury, and Southland and are restricted to basement depths or shallower. A small (27 km) crustal survey was carried out in the central South Island region (Tekapo) and used to image the base of the crust and possibly the Alpine Fault (Kleffmann et al., 1998). A more extensive survey, SIGHT98, comprised a 75-km long profile across the central part of the South Island orogen and a 35-km profile across the Alpine Fault and the west coastal plain. The shallow part of the data record a complex structure of faults and dipping strata (Long et al., 2003) in the schists of the central mountains. Although complex, the image

helps to understand the character of the inferred antithetic faulting of the convergent orogen. The deeper data (Henrys et al., 1998; also in Stern et al., Chapter XX this volume) were used to image two gently west-dipping reflectors within the mid-lower crust under the eastern part of the mountains. The lower one was inferred to mark the detachment zone between the upper crust that is being exposed at and to the east of the Alpine fault, and the lower crust that is being "subducted" into a crustal root under the Southern Alps. The data were also used to image three steeply-dipping reflectors under the western part of the Southern Alps, corresponding closely to the inferred position of the Alpine Fault (Stern et al., 2001).

vi) potential field and other data - Good regional gravity coverage exists for the South Island with stations at an average of 5 km spacing (Reilly and Whiteford, 1979). Free air, Bouguer and isostatic anomaly compilations are available. Magnetic data coverage is poor, with about 60% of the South Island, primarily the northern and southern thirds of the island, covered by high altitude (3.3 km) aeromagnetic surveys (Woodward and Hatherton, 1975; Hunt, 1978). Gravity and magnetic measurements have been made over the coastal offshore region by ships and satellite (e.g. Sutherland, 1996; Sandwell and Smith, 1997).

Gravity data have been used extensively for interpreting crustal and upper mantle structure of the Southern Alps and Alpine fault (e.g. Reilly, 1962; Woodward, 1979; Allis, 1986; Stern, 1995) and also for constraining seismic models (Eberhart-Phillips and Bannister, 2002). The Bouguer gravity field of the South Island has a number of major features (Figure 14). The two dominant features are the broad negative anomaly associated with the Southern Alps, and the large local gravity high (200 mgal) associated with the Fiordland margin. The anomaly associated with the Southern Alps reaches a minimum Bouguer anomaly of -100 mgal with the -80 mgal contour extending over a region of 200 km by 50 km. It is broader in the south and terminates east of Fiordland, although a narrow low continues to the south coast. Although the gravity anomaly appears to correspond closely with the topography, the mountains are not in isostatic equilibrium (Reilly and Whiteford 1979). The lowest negative isostatic anomaly of - 30 mgal is offset about 10 km to the southeast of the maximum topography (Woodward 1979), implying that the corresponding crustal root is offset to the southeast and/or some other forces are operating. In addition, the axis of the gravity anomaly trends off to the southeast from the plate boundary trend (e.g. Gerbault et al., 2002). These factors have been explained in several ways including

offset of the Southern Alps root to the southeast (e.g. Allis, 1986; Stern, 1995), the presence of a cold, high-density mantle blob under the Southern Alps pulling down the lithosphere (Stern et al., 2000; Scherwath et al., 2006), with subducting lithospheric roll back (Waschbusch et al., 1998), and lower crustal ductile flow towards the south (Gerbault et al., 2002).

There are no magnetic data over the central part of the Southern Alps orogen. The coverage does, however, define the trace of the Stokes magnetic anomaly/Dun Mountain ophiolite (Woodward and Hatherton,1975; Hunt, 1978). This anomaly corresponds to an obducted Permian oceanic crustal element in the Maitai terrane. It forms a major marker for the horizontal deformation of the New Zealand micro-continent since the late Mesozoic that defines the transcurrent offset on the Alpine Fault.

Heat flow data in the region are few (Figure 15). In general, heat flow is about 45 - 60 mW/m^2 but high heat flow values of about 80 - 90 mW/m^2 have been measured along the Southern Alps and in the Dunedin region (Shi et al., 1996; Funnell and Allis 1996; Cook et al., 1999). Along the Southern Alps a very high heat flow value of 190 mW/m^2 has been obtained in the region of maximum uplift near Franz Josef by Shi et al. (1996), who use this to constrain a model of the uplift and thermal state of the Southern Alps. In the Dunedin region, a high heat flow anomaly of about 90 mW/m^2 coincides with a mantle helium anomaly of up to 88% (Hoke et al., 2000).

Crustal electrical conductivity measurements have been made at several sites in the Southern Alps including a profile along transect T1 (Figure 15) using the magnetotelluric technique (Wannamaker et al., 2002; Caldwell et al., 1999; Ingham and Brown, 1998; see also Juracek et al., Chapter N17 this volume). 2D inversion of the MT data along the transect produced models showing a concave-upwards, middle to lower crustal conductivity body under the Southern Alps extending from near the Alpine Fault to about 50 km to the southeast (Wannamaker et al., 2002). In the northwest, the conductive body rises towards the Alpine Fault and becomes near-vertical about 5 km east of the fault. In the southeast the body rises to the surface coincident with a major back thrust of the orogen. Limited data to the northeast and southwest indicate that the conductive body extends along the axis of the Southern Alps.

Physical properties of rocks are available for a wide range of samples across the South Island (PETLAB data base, Mortimer, 2005; see also Christenson et al., Chapter XX this volume). These are largely density and magnetic properties but some sound velocity measurements are available. Detailed velocity measurements on a set of samples from the Southern Alps (Figure 14) showed that higher-grade schistose rocks of the Southern Alps have significant velocity anisotropy with values of up to 17 % for P waves and up to 24 % for S waves (Okaya et al., 1995; Godfrey et al., 2000).

STRUCTURE OF THE OROGEN

The development of the orogen is the result of a combination of convergent lithospheric tectonics and climate-related erosion (e.g. Adams, 1980; Koons, 1989). Lithospheric structure provides clues about the dynamic relationships among mountain uplift, lithospheric deformation, and associated uppermost mantle flow, and hence our understanding of tectonic processes. The central South Island provides an important example of the main structures and processes forming an orogen at a continental collisional plate boundary. It is the result of a relatively simple transpressive continental plate boundary that has been in existence for only the last 5 - 6 Ma.

i) broad structure (crustal, upper mantle) - In central South Island there is a simple transpressive continental plate boundary. To the north there is the influence of the Hikurangi subduction system and the associated splay faulting through northeastern South Island. To the south there is the influence of the Fiordland subducting margin, the highly uplifted Fiordland lithospheric block, and the earlier oroclinal bending of the South Island terranes. The structures, processes and influence of these regions will be discussed later. The prime data sets are the two lithospheric transects across central South Island (T1 and T2) that formed the main focus of the SIGHT experiment (Scherwath et al., 2003; Van Avendonk et al., 2004). These two transects show a number of common features (Figures 12 and 16). A prime observation is that the orogen is distinctly asymmetric at all lithospheric levels, with deformation being focussed under the eastern Pacific plate. In detail, deformation tends to be asymmetric in the crust, but symmetric within the mantle lithosphere in terms of anisotropy with respect to the plate boundary and, assuming the Stern et al., (2000) model,

accommodation of mantle shortening. However, there is also evidence here and in other transpressional plate boundary regions that the descending mantle lithosphere may be undergoing asymmetric deformation (see Fuis et al. chapter XX, this volume).

a) surface morphology. In the west, there is a narrow continental shelf, and a narrow coastal plain before the surface expression of the plate boundary - the Alpine Fault or the plate boundary thrust fault of crustal extent - is reached. This marks the base of a steep mountain front that rises to the main divide at an altitude of over 3000 m, a high intermontane region at a height of about 1500 m, largely between the main plate boundary fault and the antithetic back thrusts of the orogen (e.g. Lake Heron Fault, Cox, 1995). A major back thrust (Canterbury Range Front, Cox, 1995) marks the eastern limit of the uplifted orogen and is followed to the east by a broad outwash coastal plain and a broad continental shelf before deep water is again reached (Figures 3 and 12).

b) basement morphology-sedimentary cover. Thick (4 km) sediments underlie the western coastal strip and narrow continental shelf. They are the result of thrust loading of the Australian plate by the Pacific plate ramping up at the Alpine Fault, and deposition from high erosion of the western flanks of the Southern Alps due to high precipitation associated with the dominant westerly winds. The sedimentary stratigraphy is that of a classic foreland thrust belt (Sircombe and Kamp, 1998). To the east of the Southern Alps, thick (up to 4.5 km), broad, outwash fan deposits originating in the high alps underlie the broad coastal plain and continental shelf (Field et al., 1989).

c) crust - The crust is about 20 km thick at the extremities of the two major transects where it was thinned by rifting during the development of the continental-oceanic boundary. At the coast it thickens to about 25 - 30 km and then increases in thickness again to form an asymmetric crustal root, about 200 km wide and 40 - 50 km thick under the Southern Alps. Upper-middle crustal rocks of the Australian plate typically have seismic velocities of about 5.6 km/s at the surface ranging up to 6.1 km/s at depth. Lower crust is thin - about 1 - 4 km thick - with a seismic velocity of about 6.9 km/s. In contrast the crust of the Pacific plate has a seismic velocity of about 6.0 km/s, rising to a mid crust high-velocity layer of about 6.3 km/s at a depth of 15 km. Its lower crust is variable in thickness, thinning from about 5 km at the outboard end of the transects to almost zero at the coast, then thickening to about 10 km to form the lower part of the crustal root. Seismic velocities for the lower crust are

about 6.9 - 7.0 km/s. The crustal root is formed almost equally by thickened middle crust and thickened lower crust (Scherwath et al., 2003). Immediately east of the plate boundary, the western margin of the Pacific crust is a broad (40 km wide) low-velocity zone stretching from near the surface to the base of crust (Scherwath et al., 2003; Stern et al., 2001; Van Avendonk et al., 2004). The low-velocity zone is located in the region where the crust is being upturned along the Alpine Fault and where high anisotropy of the schists is inferred to form most of the upper-mid crust. This suggests that the low-velocity crust may be the result of anisotropy of the schists. However, teleseismic residual modelling (Stern et al., 2000) also indicates low-velocity rocks in this region. The orientation of the ray paths for the teleseismic events and for the active source survey are perpendicular, indicating isotropic rocks. Stern et al. (2001) propose over-pressured fluids derived from prograde metamorphism as the cause of the low velocities. MT data (Wannamaker et al., 2002) indicate that the low-velocity zone and mid-crust decollement are of high conductivity, and also suggest fluids derived from prograde metamorphism as the cause. Limited MT data along the strike of the Southern Alps suggest the along-axis continuation of the high-conductivity zone is a feature of the convergent plate boundary. The velocity structure in the crust is remarkably consistent among all four transects, suggesting little regional anisotropy.

Transects T1 and T2 also differ in important details (see Figure 12). Major differences can be seen in the depth of the root (deeper in T2), the dip on the western side of the root (steeper in T2), and the thickness of the lower crust in the root zone. These differences may partially be due to the different analysis techniques used; for example the dip of the Moho on the western side of the root is much less in T1 but wide-angle CDP stacked images along both profiles suggest that the dip on T1 is steeper than as modelled on the wide-angle velocity models (Henrys et al., 2004). The thickness of lower crust is important for defining how convergence is partitioned between upper and lower crust. The increased thickness of lower crust in T2 can be modelled by the obduction and erosion of upper-middle crust at the Alpine fault and by the accumulation of lower crust and lower-middle crust into the crustal root. Such a mechanism does not appear possible for the velocity structure of T1, as lower crustal material is of near-constant thickness across the crustal root region. This change can be explained by lower crustal flow towards the south (Gerbault et al.,

2002). The overall increase in the depth of the base of the crustal root to the south is consistent with the gravity data.

Differences are apparent between the active source 2D models and the 3D first-arrival tomography, particularly in the detailed structure (Figure 6, Profiles d and e, and Figure 12, Transects 1 and 2). The 2-D profiles have layered structure determined by forward modelling of arrivals from surface sources, and have additional features derived from secondary arrivals. This technique produces a detailed Moho and smooth crustal velocities within layers. The 3-D gridded inversion includes seismic sources throughout the volume and thus has more information on heterogeneity within the crust, although the Moho will be a smooth gradient over 3-10 km. The 3-D inversion uses a wide range of raypath azimuths and thus the results will show the average velocity of the volume surrounding the node, rather than an anisotropic velocity for a specific azimuth. The results of the two methods are similar, within the constraints of the techniques, which show the reliability of the results. For example, the 7.5 km/s contour would give an approximate 3-D model Moho of 40-42 km depth on the transects, similar to the forward models. The high-velocity body within the Pacific plate crust shown by the 3-D inversion is similar to that seen in the 2-D model, but it is a smoother feature with the higher velocity smeared throughout the crust. The 3-D model can thus be interpreted together with the 2-D models to examine how the Southern Alps structure varies north and south of the transects.

d) upper mantle - Uppermost mantle velocities are about 8.0 km/s under the Australian plate at the western end of the transects and about 8.1 - 8.3 km/s under the Pacific plate at the eastern end of the transects (Figure 12). For about 100 km on either side of the plate boundary, the uppermost mantle velocities are low - 7.8 km/s - along transects T1 and T2 corresponding to strong mantle rock anisotropy of up to about 11% (Scherwath et al., 2002). Under T3 off the east coast, little or no upper mantle anisotropy exists, suggesting that the eastern edge of anisotropic upper mantle is under the eastern South Island in this region. The degree and direction of anisotropy for the west coast are consistent with that obtained from shear-wave splitting (SKS) studies (Klosko et al., 1999). The anisotropy arises from the large degree of horizontal deformation (850 km over a 400 km wide zone, Sutherland, 1999) that occurred in this part of New Zealand during the Cenozoic associated with the development of the Alpine Fault.

Teleseismic data recorded along Transect 1 have been used to model a high-velocity, vertically-oriented mantle body centered about 120 km under the crustal root with its western margin immediately below the Alpine Fault (Molnar et al., 1999; Stern et al., 2000). This high-velocity region (maximum velocity anomaly of +7%) has a width of about 80 km and a vertical extent of about 100 km (Figure 9), is suggested to result from uniform thickening of mantle lithosphere. Gravity modelling is consistent with the mantle body being of higher-density rock than the surrounding lithospheric mantle, symmetrically disposed with respect to the crustal root (Stern et al., 2000), and extending well to the north and south of the transects (Scherwath et al., 2006). Uniform thickening of mantle lithosphere directly below a crustal root is consistent with growth of a Rayleigh-Taylor type of instability beneath the Southern Alps (Houseman and Molner, 1997). In contrast, the centre of the high-velocity upper mantle body of Kohler and Eberhart-Phillips (2002) lies about 40 km east of the crustal root and dips steeply to the northwest which may indicate origin from the Pacific continental mantle (Figure 9). It extends from the Hikurangi subducted slab in the north to the southern margin of South Island (Figure 10), more extensive than the major Southern Alps gravity anomaly, suggesting it may be caused, in part, by a different mechanism for accommodating mantle lithospheric shortening to that inferred by Stern et al., (2000). On the basis of limited sub-crustal seismicity in the central Southern Alps, Reyners (2005) proposes that the uppermost mantle beneath the crustal root of the Southern Alps is rigid enough to store sufficient shear strain to produce a M_W5.9 earthquake and that the pattern of seismicity is consistent with the subduction of rigid mantle. Modeling studies by Gerbault et al. (2003) also require a strong (~ 200 MPa) mantle lithosphere with an intermediate rate of strain softening. The deep (long range) reflectors recorded by the wide angle experiment off the West Coast and noted earlier, may be reflections from this upper mantle structure.

A single model for the deformation of the lithospheric mantle which can integrate the interpretations of Kohler and Eberhart-Phillips, 2002; Reyners, 2005; Stern et al., 2000) is likely a combination of both brittle and viscous deformation – plate-like behaviour in the upper part of the lithospheric mantle with distributed thickening and viscous instability in the lower part, as suggested by the modeling studies of Pysklywec et al. (2002).

ii) Constraints from other data - The depth of the brittle crust can be constrained by heat flow modelling and by seismicity. Based on limited data, modelling of the crustal thermal state under the Alps and the associated geotherms indicates a depth to the base of the crustal brittle layer (300° geotherm) of about 15 km under the east coast, thickening to about 25 km under the Southern Alps and rising to about 10 km adjacent to the Alpine Fault (Shi et al., 1996). However, a better constraint on the depth of the base of the brittle layer is defined by the maximum seismicity depths of 12 km on the flanks and 8 km under the central Southern Alps (Leitner et al., 2001). Thermal modelling also suggests the occurrence of brittle mantle seismicity to depths of about 60 km under the central Southern Alps (Shi et al., 1996), consistent with the seismicity results of Reyners (1987, 2005) and Kohler and Eberhart-Phillips (2003).

The axis of the major central South Island gravity anomaly lies at an angle of about -15° to the plate boundary (Alpine Fault), similar to the eastwards displacement of the crustal root in the south derived from seismic tomography (Eberhart-Phillips and Bannister, 2002). The data are interpreted to show a thickening and broadening of the crustal root to the south (Scherwath et al., 2006), consistent with the results of Bourguiguon et al. (Chapter XX this volume) and an increase in the gravity anomaly associated with the dense upper mantle body (Scherwath, 2002). This is compatible with a model of extrusion of highly ductile lower crustal material to the south (Gerbault et al., 2002). The model of south-directed extrusion is also consistent with plate tectonic models (Cande and Stock, 2004; Walcott, 1998) that propose greater shortening across the plate boundary in the north of the region than in the south whereas the crustal root thins to the north (Scherwath, 2002). Thickening of the lower lithosphere towards the south occurs largely in the lower crust and upper mantle and can be attributed to lower lithospheric flow arising from the transcurrent movement at the plate boundary (Gerbault et al., 2002, Scherwath et al., 2006).

iii) Regional variation (north and south) - The simple 2D structure observed in the central South Island does not continue to the north and south. This is because the simple transpressive continental tectonics are modified by other processes and inherited structures as the plate boundary changes from a transform plate boundary to west-dipping subduction in the north and east-dipping subduction in the south. In the north, the major change occurs near Arthur's Pass where the first of the northeast-trending Marlborough faults splays off to the east from the Alpine Fault and the "big

bend" in the Alpine fault trace commences. In the south, the morphology of the Southern Alps undergoes a major change in the Haast Pass region where they broaden and have reduced elevation. The plate boundary, as delineated by the Alpine Fault, becomes a subdued morphological feature. At times it shows minor uplift to the west, eventually running offshore at Milford Sound at the northern end of the Fiordland block where plate-boundary deformation comprises highly oblique, oceanic-continental subduction. These changes are reflected in the geology and gravity which show a swing in structure from northeast-southwest - parallel to the Alpine Fault and the present plate boundary - to west-northwest-east-southeast and the termination of the major gravity anomaly. In northern Fiordland, the Alpine Fault becomes aligned with the subducted slab, about 80 km northwest of the crustal root (Fig. 8c). The continuation to the south of the high-velocity, near-vertical body in the upper mantle (Kohler and Eberhart-Phillips, 2002) lies east of the subducted plate under Fiordland, and is aligned with the Solander Basin and Macquarie Ridge to the south. Whether it continues along the Macquarie Ridge strike-slip plate boundary or terminates is unknown, but it appears to be unrelated to the Fiordland subducting plate.

a) Marlborough region. The northeastern end of the plate boundary through South Island is formed by the Marlborough Fault System (Fig 1), a system of faults that splay off to the east from the Alpine Fault and along which transcurrent plate motion is transferred across Cook Strait (Lewis et al., 1994) and into the back-arc region of the North Island (Hikurangi) subduction system. The region coincides with the southern end of the zone of intermediate to deep seismicity (Anderson and Webb, 1994) associated with the Hikurangi subduction zone. Reyners and Robertson (2004) propose that the subducting Pacific plate does not stop abruptly here but instead becomes aseismic, possibly due to a change in dehydration conditions in the slab. The region also coincides with the position where the subducting slab changes from oceanic to continental as the Chatham Rise is brought into the subducting region. Eberhart-Phillips and Reyners (1997) present 3D velocity images for the region derived from the tomographic inversion of earthquake data. In the uppermost mantle they image a low-velocity zone associated with seismicity. They infer this to be related to the continental nature of the subducted plate with the increase in the amplitude of the velocity anomaly to the southwest associated with the increasing thickness of the continental crust being subducted. They suggest that subduction is relatively minor and the plate interface may be locked, leading to the intense

deformation at the coastal region. As a result of this attempt to subduct buoyant continental crust, the overriding plate has been compressed leading to the development of the Kaikoura Ranges (Inland and Seaward) with their very sharp onset at the coast (Figure 3). This overlying plate in a region that extends as far to the northwest as the Awatere Fault, is also associated with a low seismic velocity and high seismicity. It is inferred to be weak, probably as a result of elevated pore pressures caused by fluids derived from the dehydration of the subducted continental crust.

Deformation in the region is accommodated by the east-northeast-striking dextral strike-slip Marlborough Fault System, with early (Miocene and later) movement largely concentrated on the Wairau Fault in the west, where Wilson et al. (2004) infer significant crustal thinning, although this is not seen on the tomographic images of Eberhart-Phillips and Reyners (1997) perhaps because of lack of resolution in the latter. Late Quaternary slip rates on the faults increase from west to east (van Dissen and Yeats, 1991) with most of the present relative plate motion taken up on a belt of distributed shear closer to the Hikurangi Trough (Bibby, 1981). The fault azimuths change from about 70° in the south to 50° in the north as a result of increasing thrust faulting in the northeast and rapid uplift of the coastal ranges.

b) Fiordland region. The southern end of the plate boundary system runs offshore at the northern end of the Fiordland region and continues along the coast to the southern end of South Island into Puysegur Trench. Oceanic crust of the Australian plate lies to the west of the plate boundary and highly oblique subduction occurs along it. The juxtaposition of oceanic crust with very high grade metamorphic rocks onshore, along a sharp lithospheric boundary with a component of convergence, has given rise to a strong positive gravity anomaly onshore and a complementary negative anomaly offshore. The onshore part of this region also coincides with a restricted zone of intermediate depth seismicity where lower crustal seismic velocities occur very near the surface (Woodward, 1972; Davey and Broadbent, 1980; Davey and Smith, 1983; Eberhart-Phillips and Reyners, 2001) (Figs. 6b, 8a).

Recent data from a 24-station temporary array provide accurate hypocentres, focal mechanisms and 3-D velocity structure for the region. They document the change towards the southwest from lithospheric thickening under the Southern Alps to near-vertical subduction of oceanic Australian plate under Fiordland, and the transition from this near-vertical subduction to inferred lower-angle subduction of the

Australian plate at the Puysegur trench south of South Island (Eberhart-Phillips and Reyners, 2001; Reyners et al., 2002). The data were used to image a high-velocity body in the Pacific mantle which they infer has caused the subducting Australian oceanic slab to bend progressively steeper to the northeast (Fig. 8b). This interpretation follows the ploughshare or twisted subducted plate model, originally proposed by Christoffel and Van der Linden (1972), invoking a break in the subducted plate to achieve the steep dip and tight "bending" also suggested by Davey and Smith (1983). The bending is consistent with subducted plates losing most of their strength inboard of the trench (Billen and Gurnis, 2005). Malservisi et al. (2003) propose a tear along the Fiordland margin to achieve a similar effect. The present tectonics of the region are characterized by the unusual subduction environment along the Fiordland coast and the broad extensional environment to the east where subdued basin and range deformation of the pre-Cenozoic basement occurs.

CONCLUSIONS

The Pacific - Australian plate boundary through the South Island is a major transcurrent fault joining west-dipping oceanic subduction under the North Island in the north, and east-dipping, highly oblique subduction off Fiordland in the southwest. This transcurrent deformation has experienced an increasingly large amount of convergence during the past 5 Ma or so. The central part of the South Island has been taken to represent a simple, 2D convergent continental plate boundary, but more detailed investigation demonstrates that the deformation is 3D in nature, resulting from the transpressive nature of the relative plate motion. Research over the central, quasi 2D sector of the plate boundary identifies some of the major features of transpressive continental plate boundaries. The SIGHT transects illustrate these features well (Figure 16). The deformation is accommodated by the ramping up of the upper part of the Pacific plate over the Australian plate. This initially asymmetric deformation may be defined by an initial difference in lithospheric strength (Australian plate stronger than the Pacific plate, e.g. Koons, 1990, or v.v Scherwath, 2002), or an inherited suture resulting from earlier plate motions (Sutherland et al 2000). Evidence supports both explanations and the real cause may be some combination of both (e.g. Gerbault et al., 2003). The ramping up of the Pacific crust is accompanied by the delamination of the Pacific plate with the result of the uplift and

exposure of mid-crustal rocks at the plate boundary fault (Alpine Fault) forming a foreland mountain chain that has developed a particular climatic response: increased precipitation and the development of increased uplift resulting from the positive feedback loop of erosion and isostatic unloading of the underlying rocks. This is accompanied by the formation of a thick crustal root (additional 8 - 17 km) formed by the delaminated lower crust and a thickening of the overlying middle crust. Lower crust is variable in thickness both along and across the orogen. The variation may arise from pre-transpression extension away from the focus of the orogen, and convergence in and along the orogen with lower lithosphere extrusion being proposed for the latter. Low-velocity zones in the crust occur adjacent to the plate boundary (Alpine Fault) in both the Australian and Pacific plates. Fracturing of the upper crust as a result of flexural bending is proposed as the cause for the low-velocity crust in the Australian plate. The low-velocity zone in the Pacific plate at the plate boundary is suggested to be caused by high-pressure fluids in the crust derived from prograde metamorphism of the crustal rocks as they are being exhumed. This explanation is supported by high conductivity measurements in the same region from MT observations. The ramp fault and the delaminating decollement are well-imaged on seismic reflection data. First-order calculations indicate a conservation of mass within the system (Van Avendonk et al., 2004; Henrys et al., 2004). The accommodation of lithospheric mantle shortening is probably a combination of both brittle and viscous deformation. The structure of the orogen forming the Southern Alps conforms to theoretical and data-based models showing an uplifted region constrained by the major ramp fault and antithetic faulting.

ACKNOWLEDGEMENTS

We gratefully acknowledge the tremendous support of the people involved in the field work that provided the basis for this paper, in particularly in the SIGHT and SAPSE experiments. We also acknowledge funding support from NSF (grants EAR-9805224 (MDK)) and the NZ Foundation for Research Science and Technology. Reviews by Martin Reyners and Andrew Gorman were greatly appreciated.

REFERENCES

Abercrombie, R. E., T. H. Webb, R Robinson, P J McGinty, P J Mori, J R Beavan, 2000. "The engima of the Arthur's Pass, New Zealand, earthquake 1: reconciling a variety of data for an unusual earthquake sequence." *Journal of Geophysical Research 105*: 16,119-16,137.

Adams, J., 1979. Vertical drag on the Alpine Fault, New Zealand. In R.I. Walcott, M.M. Cresswell (eds), *The Origin of the Southern Alps, Bulletin 18,* Royal Society of New Zealand, Wellington, New Zealand, p47-54.

Adams, J., 1980. Contemporary uplift and erosion of the Southern Alps, New Zealand, *Geological Society of America Bulletin, vol 91(1)*, Pt1 2-4, Pt2 1-114

Allis, R.G., 1986. Mode of crustal shortening adjacent to the Alpine fault, New Zealand. Tectonics, 5, 15-32.

Anderson, H., Webb T., 1994. New Zealand seismicity: Patterns revealed by the upgraded National Seismograph Network. New Zealand journal of geology and geophysics, 37, 477-493

Anderson, H., Eberhart-Phillips, D., McEvilly, T., Wu, F. and Uhrhammer, R., 1997. Southern Alps passive seismic experiment. Institute of Geological and Nuclear Sciences Ltd science report 97/21.

Balance, P.F., 1993. The Paleo-Pacific, post-subduction, passive margin thermal relaxation sequence (Late Cretaceous-Paleogene) of the drifting New Zealand continent, in Balance. P.F., (ed) *South Pacific Sedimentary Basins, Sedimentary Basins of the World, 2,* Elsevier, Amsterdam, pp 93-110.

Barnes, P.M.; Sutherland, R.; Delteil, J. 2005 Strike-slip structure and sedimentary basins of the southern Alpine Fault, Fiordland, New Zealand. *Geological Society of America bulletin, 117(3/4):* 411-435

Bibby, H., 1981. Geodetically determined strain across the southern end of the Tonga-Kermadec-Hikurangi subduction zone.*Geophysical journal of the Royal Astronomical Society, 66(3):* 513-533

Billen M. I., Gurnis M., 2005. Constraints on subducting plate strength within the Kermadec trench, *J. Geophys. Res., 110*, B05407, doi:10.1029/2004JB003308.

Cande, S. C. and J. M. Stock, 2004. Pacific-Antarctic-Australia motion and the deformation of the Macquarie Plate. *Geophysical Journal International 167*, 399-414.

Caldwell G.T., 1999. 1998 South Island magnetotelluric transect.*Newsletter / New Zealand Geophysical Society, 49:* 32-33

Christoffel, D. A., van der Linden, W. J. M., 1972. Macquarie Ridge, New Zealand Alpine Fault transition, II: the Australian-New Zealand sector.p. 235-242 In: Hayes, D.E. (ed.) *Antarctic Oceanology*. Washington: American Geophysical Union. Antarctic research series 19

Cook, R.A.; Sutherland, R.; Zhu, H. 1999: Cretaceous-Cenozoic geology and petroleum systems of the Great South Basin, New Zealand. *Institute of Geological & Nuclear Sciences Monograph:* 188 p.

Cox, S.C., 1995. Geological transect across the Southern Alps of New Zealand, *Institute of Geological and Nuclear Sciences science report 95/30*, Institute of Geological & Nuclear Sciences Ltd, Lower Hutt, New Zealand, 32 p.

Davey F J., Smith, E G C., 1983. The tectonic setting of the Fiordland region. *Geophysical Journal of the Royal Astronomical Society 72:* 23-28.

Davey, F. J., Broadbent, M., 1980. Seismic refraction measurements in Fiordland, southwest New Zealand, *New Zealand journal of geology and geophysics, 23*, 395-406

Davey, F.J., Henyey, T., Holbrook, W.S., Okaya, D, Stern T.A., Melhuish, A., Henrys, S., Eberhart-Phillips, D., McEvilly, T., Urhammer, R., Anderson, H., Wu, F., Jiracek, G., Wannermaker, P., Caldwell, G., and Christensen, N., 1998. Preliminary results from a geophysical study across a modern continent-continent

collisional plate boundary - the Southern Alps, New Zealand. *Tectonophysics, 288*, 221-235.

Davey, F. J., 2005. A Mesozoic crustal suture on the Gondwana margin in the New Zealand region.*Tectonics, 24(4):* TC4006, doi:1029/2004TC001719

Eberhart-Phillips, D., Henderson, C.M., 2004. Including anisotropy in 3-D velocity inversion and application to Marlborough, New Zealand. *Geophysical journal international, 156(2):* 237-254.

Eberhart-Phillips, D.; Reyners, M.E. 1997 Continental subduction and three-dimensional crustal structure : the northern South Island, New Zealand. *Journal of geophysical research, 102(B6)*: 11843-11861

Eberhart-Phillips, D. and M. E. Reyners, 2001. "A complex, young subduction zone imaged by three-dimensional seismic velocity, Fiordland, New Zealand." *Geophysical journal international* 146(3): 731-746.

Eberhart-Phillips, D. and S. C. Bannister, 2002. "Three-dimensional crustal structure in the Southern Alps region of New Zealand from inversion of local earthquake and active source data." *Journal of geophysical research. Solid earth* 107(B10): doi:10.1029/2001JB000567.

Field, B.D.; Browne, G.H.; Davy, B.W.; Herzer, R.H.; Hoskins, R.H.; Raine, J.I.; Wilson, G.J.; Sewell, R.J.; Smale, D.; Watters, W.A. 1989. Cretaceous and Cenozoic sedimentary basins and geological evolution of the Canterbury region, South Island, New Zealand.Lower Hutt: New Zealand Geological Survey. *New Zealand Geological Survey basin studies 2.* 94 p.

Funnell, R.H., Allis, R.G., 1996. Hydrocarbon maturation potential of offshore Canterbury and Great South Basins, in *1996 New Zealand Petroleum Conference proceedings vol 1*, Ministry of Commerce, Wellington, 22-30.

Gerbault, M., F. J. Davey, S. A. Henrys, 2002. "Three-dimensional lateral crustal thickening in continental oblique collision; an example from the Southern Alps, New Zealand." *Geophysical Journal International* **150**(3): 770-779.

Gerbault, M., S. A. Henrys, F. J. Davey, 2003. Numerical models of lithospheric deformation forming the Southern Alps of New Zealand, *J. Geophys. Res. 108* (B7 2341):doi: 10.1029/2002JB001716.

Godfrey, N. J., N. I. Christensen, et al., 2000. Anisotropy of schists: contributions of crustal anisotropy to active-source seismic experiments and shear-wave splitting observations. *J. Geophys. Res. 105*: 27991-28007.

Godfrey, N. J., F. Davey, et al., 2001. Crustal structure and thermal anomalies of the Dunedin region, South Island, New Zealand. *Journal of Geophysical Research, B, Solid Earth and Planets 106(12)*: 30,835-30,848.

Greenroyd, C. Yu, J. Melhuish, A. Ravens, J.M. Davey, F. Maslen, G. SIGHT WORKING GROUP, (2003). New Zealand South Island GeopHysical Transect (SIGHT): Marine active-source seismic component - a processing summary. *Institute of Geological & Nuclear Sciences science report 2003/04*.

Hatherton, T., 1980. Shallow seismicity in New Zealand 1956-75, *Journal of Royal Society of New Zealand, 10*, 19-25.

Henrys, S.A.; Okaya, D.; Melhuish, A.; Stern, T.A.; Holbrook, S. 1998 Near-vertical seismic images of a continental transpressional plate boundary : Southern Alps, New Zealand.*Eos, 79(45:supplement):* F901

Henrys, S. A., D. J. Woodward, D Okaya, J Yu, 2004. Mapping the Moho beneath the Southern Alps continent-continent collision, New Zealand, using wide-angle reflections. *Geophysical research letters 31(17):* L17602, doi:1029/2004GL020561.

Hoke, L., R. Poreda, Reay, A. Weaver, S. D., 2000. The subcontinental mantle beneath southern New Zealand characterised by helium isotopes in intraplate basalts and gas-rich springs. *Geochim. Cosmochim. Acta 64*: 2489-2507.

Houseman, G A., and P. Molnar, 1997. Gravitational (Rayleigh-Taylor) instability of a layer with non-linear viscosity and convective thinning of continental lithosphere, *Geophys. J. Int., 128*, 125-150.

Hunt, T., 1978. Stokes magnetic anomaly system. *New Zealand journal of geology and geophysics, 21(5)*: 595-606

Ingham, M.; Brown, C. 1998. A magnetotelluric study of the Alpine Fault, New Zealand.*Geophysical journal international, 135(2):* 542-552

Kleffmann, S., 1999. Crustal structural studies of a transpressional plate boundary : the central South Island of New Zealand. PhD (Geophysics) thesis, Victoria University of Wellington

Kleffmann, S., F. Davey, Melhuish, A. Okaya, D. Stern, T., 1998. Crustal structure in central South Island from the Lake Pukaki seismic experiment. *New Zealand Journal of Geology and Geophysics 41*: 39-49.

Klosko, E.R.; Wu, F.T.; Anderson, H.J.; Eberhart-Phillips, D.; McEvilly, T.V.; Audoine, E.; Savage, M.K.; Gledhill, K.R. 1999 Upper mantle anisotropy in the New Zealand region. *Geophysical Research Letters, 26(10):* 1497-1500

Kohler, M. D. and D. Eberhart-Phillips, 2002. Three-dimensional lithospheric structure below the New Zealand Southern Alps, *J. Geophys. Res*., *107(B10),* 2225, doi:10.1029/2001JB000182.

Kohler, M. D. and D. Eberhart-Phillips, 2003. Intermediate-depth earthquakes in a region of continental convergence: South Island, New Zealand, *Bull. Seis. Soc. Am., 93,* 85-93.

Koons, P. O., 1989. The topographic evolution of collisional mountain belts: a numerical look at the Southern Alps, New Zealand, *American Journal of Science, 289*, 1041-1069.

Koons, P. O., 1990. Two-sided orogen: Collision and erosion from the sandbox to the Southern Alps, New Zealand, *Geology, 18*, 679-682.

Leitner, B.; Eberhart-Phillips, D.; Anderson, H.; Nabelek, J.L. 2001: A focused look at the Alpine Fault, New Zealand: seismicity, focal mechanisms, and stress observations. *Journal of Geophysical Research 106*: 2193–2220.

Lewis, K.B.; Carter, L.; Davey, F.J. 1994 The opening of Cook Strait : interglacial tidal scour and aligning basins at a subduction to transform plate edge.*Marine geology, 116(3/4):* 293-312

Long, D.T.; Cox, S.C.; Bannister, S.C.; Gerstenberger, M.C.; Okaya, D., 2003 Upper crustal structure beneath the eastern Southern Alps and the Mackenzie Basin, New Zealand, derived from seismic reflection data. *New Zealand journal of geology and geophysics, 46(1)*: 21-39.

Malservisi, R., Furlong, K.P., Anderson, H., 2003. Dynamic uplift in a transpressional regime: numerical model of the subducted area of Fiordland, New Zealand, *Earth and Planetary Letters, 206*, 349-364.

Melhuish A, Holbrook W S, Davey F, Okaya D A., Stern T., 2004. Crustal and upper mantle seismic structure of the Australian Plate, South Island, New Zealand. *Tectonophysics 395,* 113-135, doi:10.1016/j.tecto2004.09.005.

Melhuish, A., R. Sutherland, Davey, F.J. Lamarche, G., 1999. Crustal structure and neotectonics of the Puysegur oblique subduction zone, New Zealand. *Tectonophysics 313(4):* 335-362.

Molnar, P., H. J. Anderson, E. Audoine, D. Eberhart-Phillips, K. R. Gledhill, E. R. Klosko, T. V. McEvilly, D. Okaya, M. K. Savage, T. Stern, and F. T. Wu, 1999. Continuous deformation versus faulting through the continental lithosphere of New Zealand, *Science, 286*, 516-519.

Mortimer, N. 2005 PETLAB : New Zealand's rock and geoanalytical database. *Newsletter / Geological Society of New Zealand, 136*: 27-31

Mortimer, N., Davey, F.J., Melhuish, A., Yu, J., Godfrey, N.J., 2002. Geological interpretation of a deep seismic reflection profile across the Eastern Province and Median Batholith, New Zealand: crustal architecture of an extended Phanerozoic orogen, *New Zealand Journal of Geology and Geophysics, 45*, 349-363.

Nathan, S., Anderson, H.J., Cook, R.J., Herzer, R.H., Hoskins, R.H., Raine, J.I., Smale, D. 1986. Cretaceous and Cenozoic sedimentary basins of the West Coast region, South Island, New Zealand. *New Zealand Geological Survey basin studies 1.*, New Zealand Geological Survey, Lower Hutt.

Okaya, D.; Christensen, N.; Stanley, D.; Stern, T. 1995 Crustal anisotropy in the vicinity of the Alpine Fault Zone, South Island, New Zealand.*New Zealand journal of geology and geophysics, 38(4):* 579-583

Pulford, A., Savage, M., Stern, T., 2003. Absent anisotropy: The Paradox of the Southern Alps orogen, *Geophysical Research Letters, 30(20)*, 2051, doi:10.1029/2003GL017758.

Pysklywec, R.N., Beaumont, C., Fullsack, P., 2002. Lithospheric deformation during the early stages of continental collision: numerical experiments and comparison with South Island, New Zealand, *J Geophys. Res., 107(B7),* doi:10.1029/2001JB000252.

Reyners, M., 1987. Subcrustal earthquakes in the central South Island, New Zealand, and the root of the Southern Alps, *Geology,* **15**, 1168-1171.

Reyners, M. 1988. Reservoir-induced seismicity at Lake Pukaki, New Zealand.*Geophysical journal of the Royal Astronomical Society, 93(1):* 127-135.

Reyners, M., 1989. New Zealand seismicity 1964-87: an interpretation, *New Zealand Journal of Geology and Geophysics, 32,* 307-315.

Reyners, M., 2005. The 1943 Lake Hawea earthquake - A large subcrustal event beneath the Southern Alps of New Zealand, *New Zealand journal of Geology and Geophysics, 48(1)*, 147-152.

Reyners, M. and H. Cowan, 1993. The transition from subduction to continental collision : crustal structure in the North Canterbury region, New Zealand, *Geophys. J. Int. 115(3):* 1124-1136.

Reyners, M.E.; Robinson, R.; Pancha, A.; McGinty, P.J. 2002 Stresses and strains in a twisted subduction zone : Fiordland, New Zealand. *Geophysical journal international, 148(3):* 637-648.

Reyners, M. and Robertson, E., 2004. Intermediate depth earthquakes beneath Nelson, New Zealand, and the southwest termination of the subducted Pacific plate, *Geophysical Research Letters, 31*, L04607, doi:10.1029/2003GL019201.

Reilly, W.I. 1962. Gravity and crustal thickness in New Zealand. *New Zealand journal of geology and geophysics, 5(2):* 228-33

Reilly, W.I.; Whiteford, C.M. 1979. South Island: Bouguer anomalies. Wellington: DSIR. *Gravity map of New Zealand 1:1,000,000* . 1 map

Sandwell, D. T. and W. H. F. Smith, 1997. Marine gravity anomaly from Geosat and ERS 1 satellite altimetry. *Journal of Geophysical Research, B, Solid Earth and Planets 102(5)*: 10,039-10,054.

Savage, M. K., 1999. Seismic anisotropy and mantle deformation: What have we learned from shear wave splitting? *Rev. Geophys. 37*: 65-106.

Scherwath, M., 2002. Lithospheric structure & deformation in an oblique continental collision zone, South Island, New Zealand, PhD thesis, Victoria University of Wellington, Wellington, New Zealand.

Scherwath, M., Stern, T., Melhuish, A., Molnar, P., 2002. Pn anisotropy and distributed upper mantle deformation associated with a continental transform fault, *Geophys. Res. Lett., 29(8)*10.1029/2001GLO14179.

Scherwath, M., T. Stern, Davey, F. Okaya, D. Holbrook, W. S. Davies, R. Kleffmann, S., 2003. Lithospheric structure across oblique continental collision in New Zealand from wide-angle P wave modeling. *Journal of Geophysical Research, B, Solid Earth and Planets 108(B12)*: doi:10.1029/2002JB002286.

Scherwath, M., Stern, T., Davey, F., Davies, R., 2006. Three-dimensional lithospheric deformation and gravity anomalies associated with oblique continental collision in South Island, New Zealand. *Geophys. J. Int. 167*, 906–916, doi: 10.1111/j.1365-246X.2006.03085.

Shi, Y., R. Allis, F Davey, 1996. Thermal modeling of the Southern Alps, New Zealand. *Pure and applied geophysics 146(3/4):* 469-501.

Sircombe, K.N.; Kamp, P.J.J., 1998. The South Westland Basin : seismic stratigraphy, basin geometry and evolution of a foreland basin within the Southern Alps collision zone, New Zealand. *Tectonophysics, 300(1/4):* 359-387.

Smith, E.G.C., Stern, T., O'Brien, B., 1995. A seismic velocity profile across the central South Island, New Zealand, from explosion data. *New Zealand journal of geology and geophysics, 38*, 565-570.

Stern, T. A., (1995). Gravity anomalies and crustal loading at and adjacent to the Alpine Fault, New Zealand. In Origin of the Southern Alps II. *Origin of the Southern Alps symposium 38(4)*: 593-600.

Stern, T. A., P. E. Wannamaker, D. Eberhart-Phillips, D. Okaya, F. J. Davey, and S. I. P. W. Group, 1997. Mountain building and active deformation studied in New Zealand, *Eos, Transactions, American Geophysical Union*, *78*, 329,335-336.

Stern, T., P. Molnar, D. Okaya, and D. Eberhart-Phillips, 2000. Teleseismic P wave delays and modes of shortening the mantle lithosphere beneath South Island, New Zealand, *J. Geophys. Res*., *105*, 21,615-21,631.

Stern, T., S. Kleffmann, Okaya, D, Scherwath, M, Bannister, S. 2001. Low seismic-wave speeds and enhanced fluid pressure beneath the Southern Alps of New Zealand. *Geology (Boulder) 29(8):* 679-682.

Suggate, P.R., Stevens, G.R. Te Punga, M.T., (Editors), 1978. *The Geology of New Zealand.* N.Z. Government Printer, Wellington, 2 vols.

Sutherland, R. 1996. Gravity anomalies and magnetic lineations in the South Pacific, 1:15,000,000.Lower Hutt: Institute of Geological & Nuclear Sciences. *Geophysical map / Institute of Geological & Nuclear Sciences 10.* 1 map.

Sutherland, R., 1999. Cenozoic bending of New Zealand basement terranes and Alpine Fault displacement: A brief review. *N. Z. J. Geol. Geophys., 42*, 295-301

Sutherland, R., F. Davey, and J. Beavan, 2000. Plate boundary deformation in South Island, New Zealand, is related to inherited lithospheric structure, *Earth Plan. Sci. Lett., 177*, 141-151.

Sutherland, R.; Melhuish, A., 2000. Formation and evolution of the Solander Basin, southwestern South Island, controlled by a major fault in continental crust and upper mantle. *Tectonics 19*: 44–61.

Townend, J., 1997. Estimates of conductive heat flow through bottom-simulating reflectors on the Hikurangi margin and southwest Fiordland, New Zealand. *Mar. Geol. 141*: 209-220.

Van Avendonk, H. J. A., W. S. Holbrook, Okaya, D. Austin, J. K. Davey, F. Stern, T., 2004. Continental crust under compression: a seismic refraction study of SIGHT Transect I, South Island, New Zealand. *Journal of Geophysical Research, B, Solid Earth and Planets 109(B6)*: doi10.1029/2003JB002790.

Van Dissen, R.; Yeates, R.S., 1991. Hope fault, Jordan thrust, and uplift of the Seaward Kaikoura Range, New Zealand. *Geology, 19:* 393-396.

Walcott, R. I., 1998. Modes of oblique compression; late Cenozoic tectonics of the South Island of New Zealand. *Reviews of Geophysics 36(1):* 1-26.

Wannamaker, P. E., G. R. Jiracek, J. A. Stodt, T. G. Caldwell, V. M. Gonzalez, J D. McKnight, A. D. Porter, 2002. Fluid generation and pathways beneath an active compressional orogen, the New Zealand Southern Alps, inferred from magnetotelluric data. *Journal of Geophysical Research, B, Solid Earth and Planets 107(6)*: 22.

Waschbusch, P., Batt, G., Beaumont, C., 1998. Subduction zone retreat and recent tectonics of the South Island of New Zealand, *Tectonics, 17(2),* 267-284.

Wellman, H. W., 1979. An uplift map for the South Island of New Zealand, and a model for uplift of the Southern Alps. In R.I. Walcott, M.M. Cresswell (eds), *The Origin of the Southern Alps, Bulletin 18,* Royal Society of New Zealand, Wellington, New Zealand, p13-20.

Wilson, C.K., Jones, C.H., Molnar, P., Sheehan. A.F., Boyd, O.S., 2004. Distributed deformation in the lower crust and upper mantle beneath a continental strike-slip fault zone: Marlborough fault system, South Island, New Zealand, *Geology, 32(10),* 837–840; doi: 10.1130/G20657

Wilson, D.; Eberhart-Phillips, D. 1998 Estimating crustal thickness in the central South Island.Lower Hutt: Institute of Geological & Nuclear Sciences. *Institute of Geological & Nuclear Sciences science report 98/27.* 61 p.

Wood, R.A.; Herzer, R.H.; Sutherland, R.; Melhuish, A. 2000 Cretaceous-Tertiary tectonic history of the Fiordland margin, New Zealand.*New Zealand journal of geology and geophysics, 43(2):* 289-302

Woodward, D.J. 1972 Gravity anomalies in Fiordland, south-west New Zealand.*New Zealand journal of geology and geophysics, 15(1):* 22-32

Woodward, D.J., 1979. The crustal structure of the Southern Alps, New Zealand, as determined by gravity.p. 95-98 In: Walcott, R.I. (eds.); Cresswell, M.M. (eds.) *The origin of the Southern Alps*. Bulletin Royal Society of New Zealand 18, Royal Society of New Zealand, Wellington.

Woodward, D.J.; Hatherton, T., 1975. Magnetic anomalies over southern New Zealand. *New Zealand journal of geology and geophysics, 18(1)*: 65-82.

Zelt, C. A. and R. B. Smith, 1992. Seismic traveltime inversion for 2-D crustal velocity structure. *Geophysical Journal International 108*: 16-34.

.

FIGURE CAPTIONS

Figure 1 The plate tectonic setting of the New Zealand region, showing the morphology (color scale) and plate boundary through the region (solid line). Subduction boundaries (Hikurangi and Puysegur) are marked by solid line and triangles, transcurrent boundary (Alpine fault) by a dotted line, and convergence direction and rate by the annotated arrow. The location of Figures 2, 11, 14 and 15 are shown by the box.

Figure 2 Locations and topography of the South Island region (grey scale illuminate from the northeast). The Alpine fault and Marlborough faults marked by the thin lines. The topographic profiles (a, b and c) in Figure 3 are located by the thick lines.

Figure 3 Topographic profiles across the South Island: a) northern, b) central Southern Alps, c) southern. AF marks the location of the Alpine Fault. Regions i - v in (b) are discussed in the text. Note the broadening of the high topography in the northern and southern regions of South Island, plus the northern region's steep eastern margin.

Figure 4. Seismicity of South Island from the New Zealand National Seismograph Network (NZNSN). a) Moderate-to-large earthquakes, $M_L \geq 5.8$, 1840-2002. $M_L \geq 3.0$, 1990-2002: b) crustal seismicity, 0-20 km depth; c) lower crust/upper mantle, 25-60 km depth; d) slab, 90-250 km depth. Squares = NZNSN stations.

Figure 5. Shallow central South Island seismicity (Leitner et al., 2001). Maps showing quality locations of SAPSE (solid circles), Pukaki (shaded circles) and NZNSN (open circles) earthquakes. (a) $M_L > 3$. Large shaded circles are $M_L > 5$ earthquakes since 1920. Note that larger earthquakes follow the seismicity patterns for the smaller earthquakes. (b) $M_L > 1.8$. HF marks the Hope Fault.

Figure 6. South Island 3-D P-velocity incorporating Southern Alps (Eberhart-Phillips and Bannister, 2002), Marlborough (Eberhart-Phillips and Reyners, 1997) and Fiordland (Eberhart-Phillips and Reyners, 2001). Mapviews at (a) 6-km depth, (b) 14-km depth, and (c) 30-km depth. White lines show low-velocity zone, M= high-velocity underlying Mackenzie basin (Fig 6b). Orientation is parallel to Alpine fault, with coastline and active faults shown, star=Mt Cook. Location map marks location of cross sections. Line marked "Marlborough" locates profile in Figure 7 across Marlborough. Lines marked "Fr-a" through "-c" locate profiles shown in Figure 8. WF - Wairau Fault, AF Awatere Fault.
(d)-(g) Y cross-sections. Dip of Alpine fault is not known, so both vertical and dipping lines (generally following a crustal low velocity zone) are shown. Locations are indicated for the Alpine fault (AF), Porters Pass fault zone (PPFZ), Forest Creek fault (FCF), Mt. Cook, Irishman's Creek fault (ICF). White lines in (f)= reflectors from SIGHT98 CDP line (see Stern at al., Chapter NN this volume).

Figure 7. Cross-section of Marlborough P-velocity from inversion including azimuthal (hexagonal) anisotropy, with shear-wave splitting initial model (Eberhart-Phillips and Henderson, 2004), location indicated in Fig. 6. Isotropic component of Vp is shown by grey-scale and contoured at 0.25 km/s. Bars at each node show the magnitude and fast azimuth of azimuthal anisotropy. These are 2-D azimuths even on cross-sections, ie: vertical bar = north azimuth and horizontal bar = east azimuth. The maximum magnitude in each plot is specified. Hypocenters are shown by pluses. Abbreviations are as follows: Aw, Awatere fault; Cl, Clarence fault; H, Hope fault; Kr, Karamea fault; Wm, Waimea fault; and Wr, Wairau fault. Note no significant crustal thinning across the Wairau Fault.

Figure 8. Tectonic interpretation of 3-D velocity model (Eberhart-Phillips and Reyners, 2001), cross-sections as indicated in Fig. 6. a) Moderate-dip subduction occurs in the southern part of Fiordland. b) North of Doubtful Sound, the subducted slab is bent to vertical by a high-velocity body in the Pacific mantle and partitioned slip occurs on the shallow plate interface and the Alpine fault. c) North of Milford Sound, the Alpine fault becomes the lithospheric boundary to the Australian plate, and oblique convergence forms the Southern Alps. Locations are indicated for: the Alpine

fault, Hollyford fault, Moonlight fault, Dusky fault (DSF), Hauroko fault (HF), and Lake Te Anau. * - coastline.

Figure 9 Upper mantle high-velocity anomaly under the South Island. Vertical section of the mantle velocity anomaly along SIGHT transects 1 and 2. The grey shaded contours are of % velocity perturbation from a velocity of 8.2 km/s, after Kohler and Eberhart-Phillips (2002), and are overlain by dashed contours of the mantle velocity model (0.1 km/s intervals with a base level of 8.1 km/s) after Stern et al. (2000). The Kohler and Eberhart-Phillips "slab" dips steeply northwest through the centre of the Stern et al. "blob"

Figure 10 Depth slices at 100 km and 180 km depth of velocity anomaly, after Kohler and Eberhart-Phillips (2002), showing the continuity of the high-velocity slab from southern North Island to off the central south coast of South Island and its position relative to the surface position of the Alpine fault.

Figure 11 The location of profiles of the SIGHT project overlain on a generalised geology of the South Island. The two main transect of SIGHT each comprise a land transect and their extension offshore to east and west. Tie lines are formed by Transect 3 (line 4e, a land component and line 6e) and line 3w. The Alpine fault and Marlborough splay faults to the north are also shown.

Figure 12 Velocity models along a) Transect 1 (Van Avendonk et al., 2004), b) Transect 2 (Scherwath et al., 2003), c) Transect 3 (Godfrey et al., 2001), d) Line 3w (Melhuish et al., 2005). Velocity contours are in km/s and also shown by a broad grey scale. Note the distinct asymmetry of the orogen. AF - Alpine Fault, LHF - Lake Heron Fault, RFF - Range Front Fault.

Figure 13 Seismic reflection profile SIGHT line 6e off southeast South Island, showing the highly variable thickness of the reflective lower crust, the sharp Moho and the large changes in its depth

Figure 14 Bouguer anomaly of the South Island (grey scale (25 mgal intervals) with contours at 50 mgal intervals) after Reilly & Whiteford (1979), showing the

large negative Bouguer anomaly associated with the Southern Alps, that trends away from the Alpine fault, and the large positive anomaly associated with the Fiordland region (southwest South Island). The two main SIGHT transects (white stars - shot locations) and the location of the offshore profiles (black stars - OBS locations) are marked.

Figure 15 Location of measurements of heat flow (solid circles, after Shi et al. 1996, Funnell and Allis 1996), MT (open diamonds, after Wannamaker et al. 2002, Caldwell pers. comm.) and detailed petrophysics data (crosses after Okaya et al. 1995) in the South Island. Heat flow values are annotated. Note high heat flow associated with the Alpine fault culminating with a maximum value of 190 mW/m^2 in the central region.

Figure 16 Lithospheric cross section and upper mantle velocity anomaly across the Southern Alps orogen (after Scherwath 2002 Figure 7.7), showing the major structural/tectonic features of the orogen.

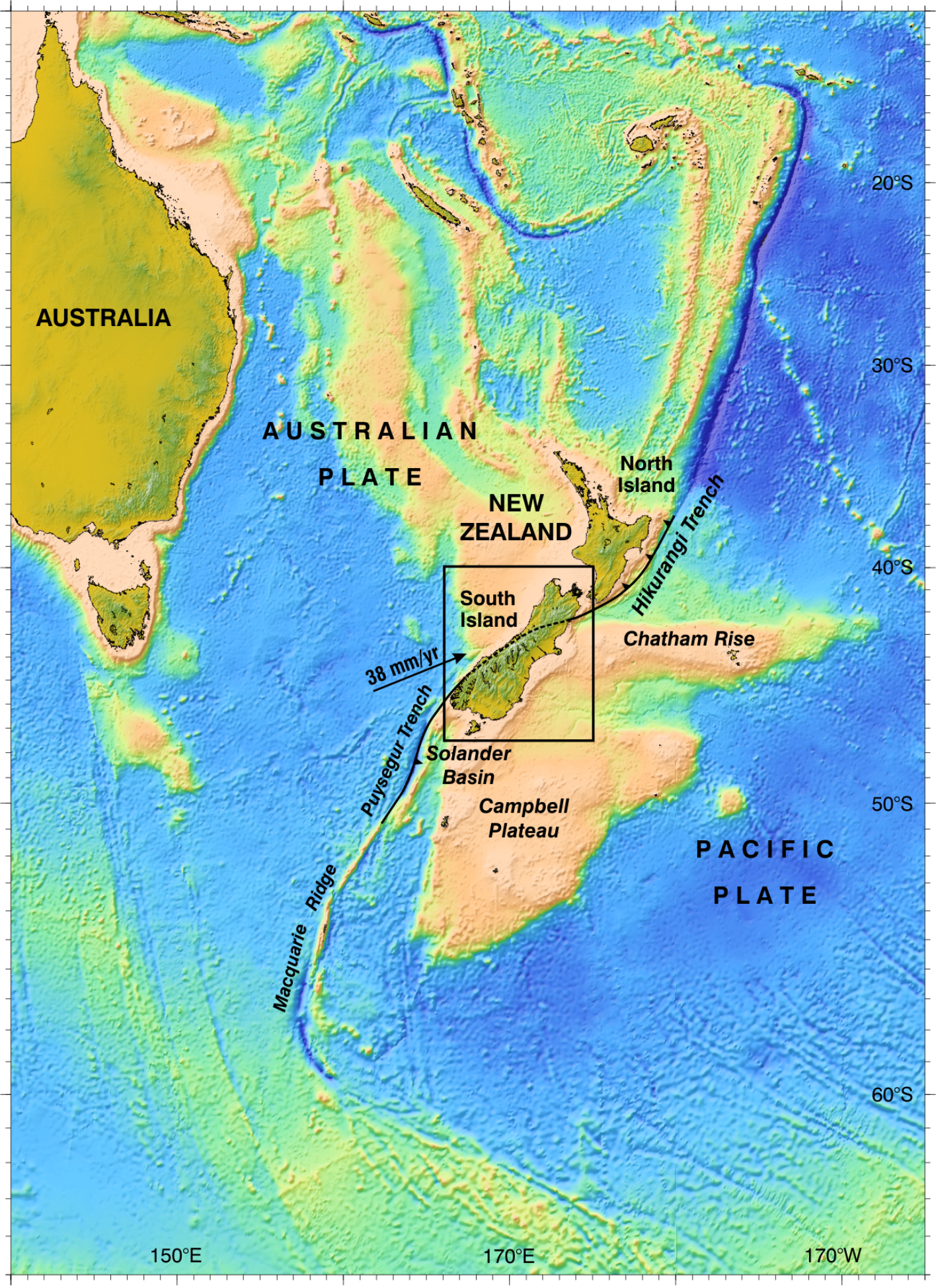
AUSTRALIA
AUSTRALIAN
PLATE
NEW
ZEALAND
North
Island
South
Island
Hikurangi Trench
Chatham Rise
38 mm/yr
Puysegur Trench
Solander
Basin
Campbell
Plateau
PACIFIC
PLATE
Macquarie Ridge
20°S
30°S
40°S
50°S
60°S
150°E
170°E
170°W
-10000
-5000
-3000
-1000
0
1000
3000
Elevation (metres)

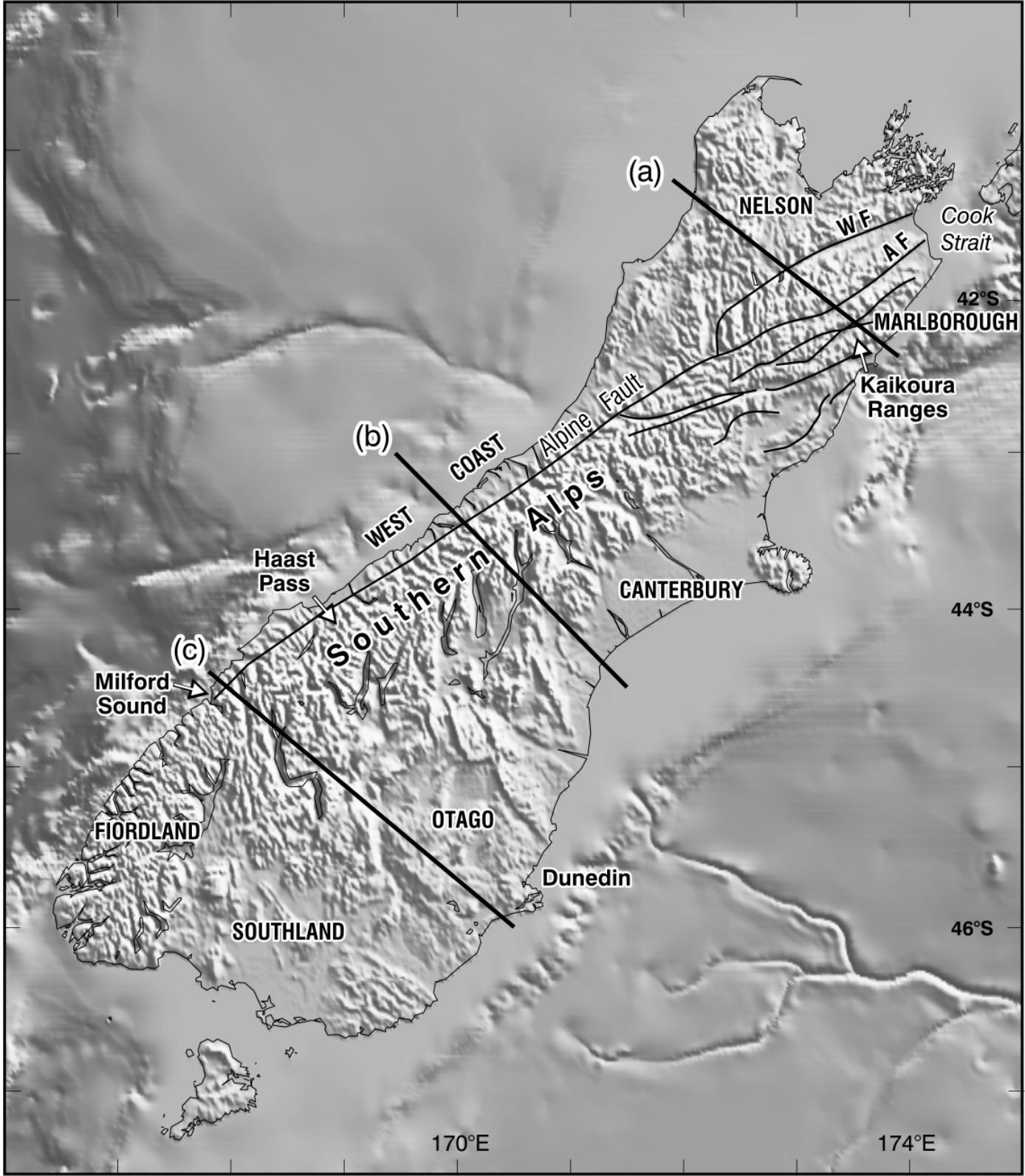
(a)
NELSON
WF
AF
Cook
Strait
42°S
MARLBOROUGH
Kaikoura
Ranges
Alpine Fault
(b)
COAST
WEST
Southern Alps
Haast
Pass
CANTERBURY
44°S
(c)
Milford
Sound
OTAGO
FIORDLAND
Dunedin
SOUTHLAND
46°S
170°E
174°E

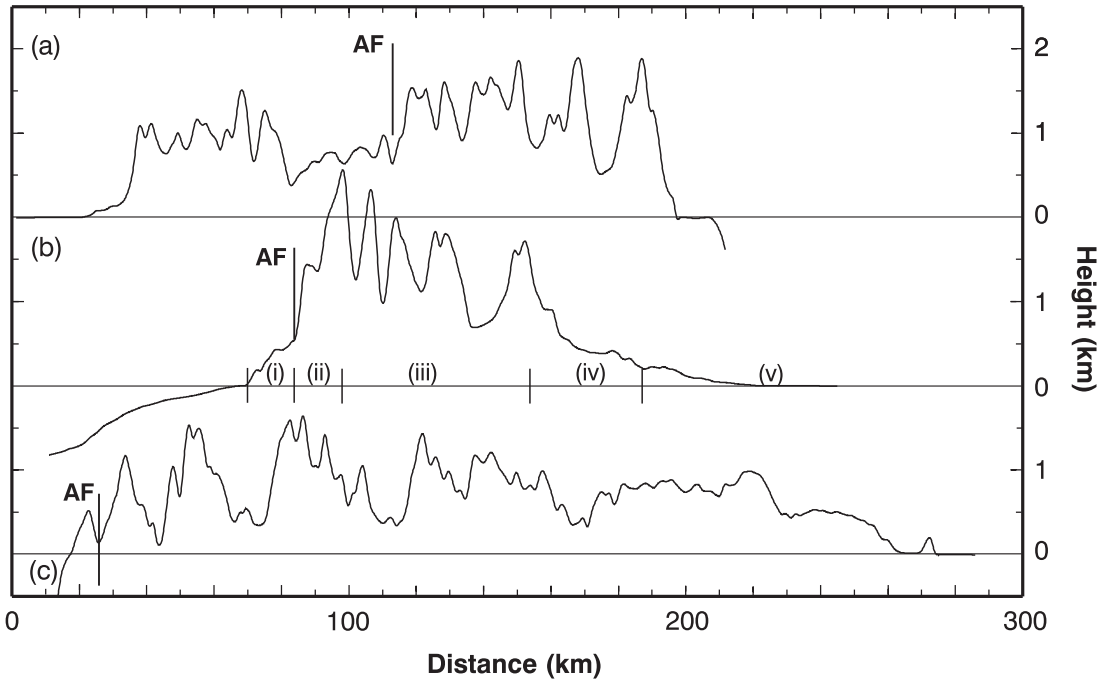
(a)
AF
(b)
AF
(i)
(ii)
(iii)
(iv)
(v)
AF
(c)
2
1
0
1
0
1
0
Height (km)
0
100
200
300
Distance (km)

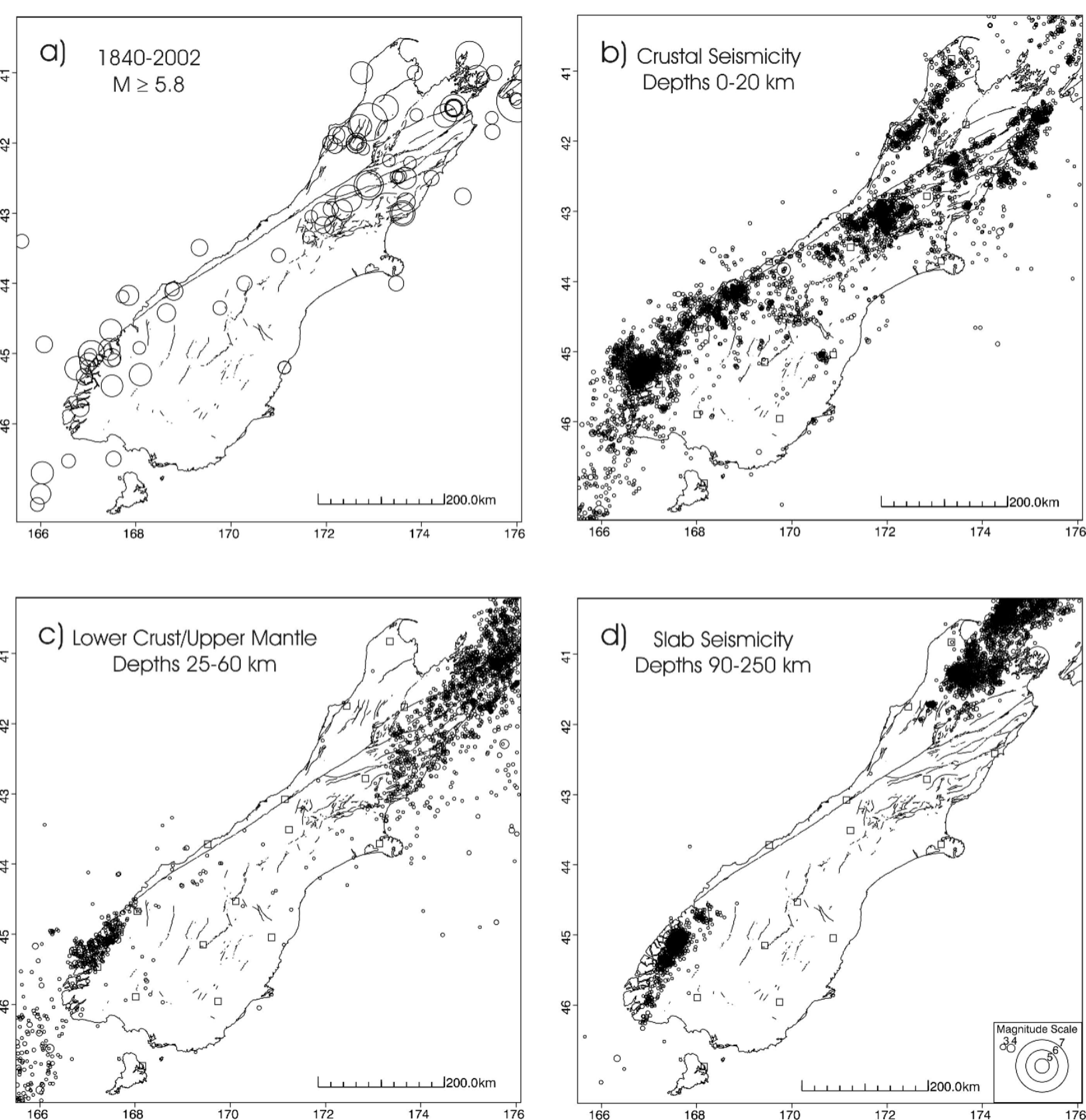
a) 1840-2002
M ≥ 5.8
b) Crustal Seismicity
Depths 0-20 km
c) Lower Crust/Upper Mantle
Depths 25-60 km
d) Slab Seismicity
Depths 90-250 km
200.0km
Magnitude Scale
3
4
5
6
7
41
42
43
44
45
46
166
168
170
172
174
176

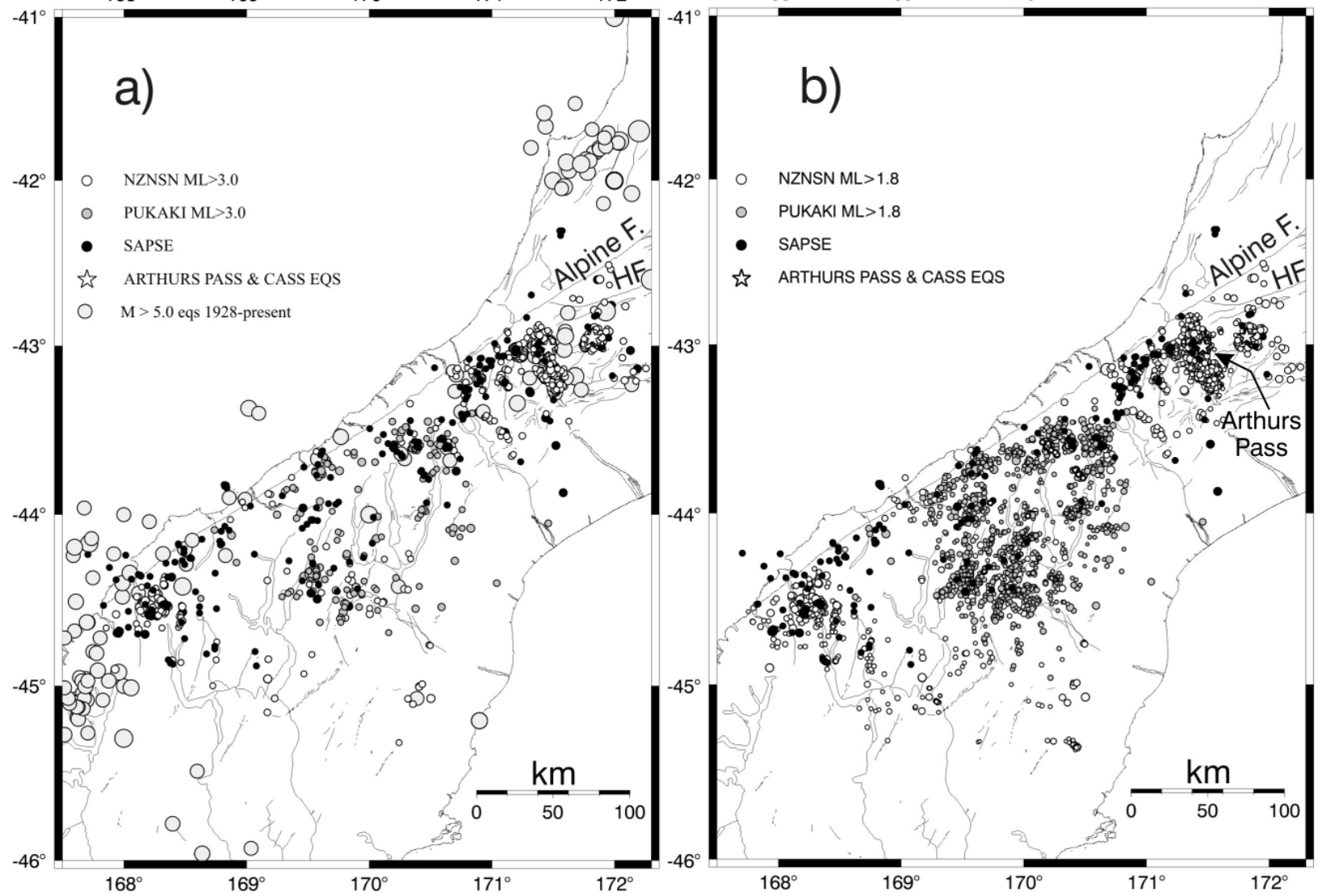
a)
NZNSN ML>3.0
PUKAKI ML>3.0
SAPSE
ARTHURS PASS & CASS EQS
M > 5.0 eqs 1928-present
Alpine F.
HF
km
0 50 100
b)
NZNSN ML>1.8
PUKAKI ML>1.8
SAPSE
ARTHURS PASS & CASS EQS
Alpine F.
HF
Arthurs Pass
km
0 50 100
-41°
-42°
-43°
-44°
-45°
-46°
168°
169°
170°
171°
172°

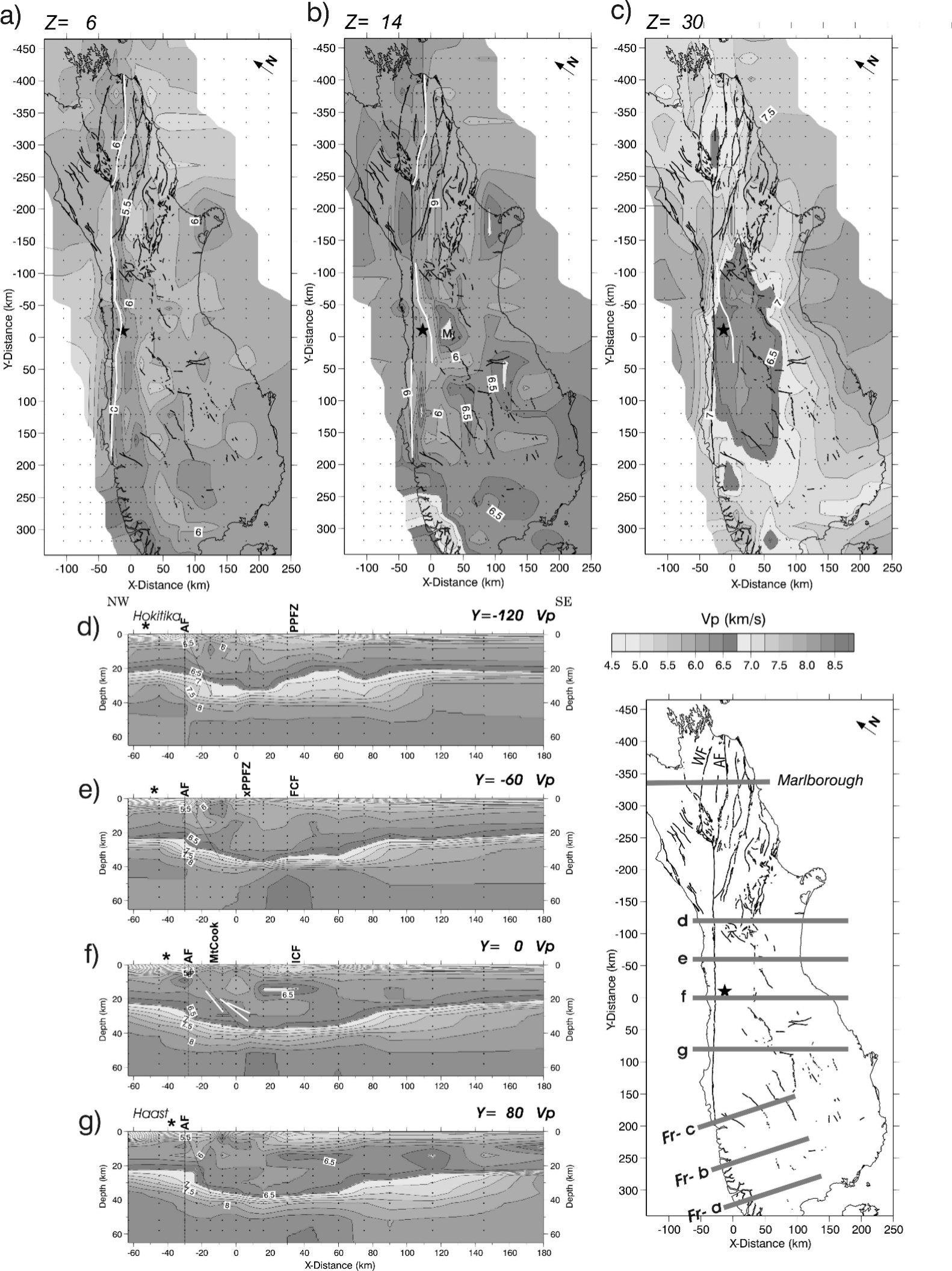
a) Z= 6
b) Z= 14
c) Z= 30
N
Y-Distance (km)
X-Distance (km)
NW
SE
d) Hokitika
Y=-120 Vp
e) Y= -60 Vp
f) Y= 0 Vp
g) Haast
Y= 80 Vp
AF
PPFZ
xPPFZ
FCF
MtCook
ICF
Depth (km)
Vp (km/s)
4.5 5.0 5.5 6.0 6.5 7.0 7.5 8.0 8.5
WF
Marlborough
Fr- c
Fr- b
Fr- a

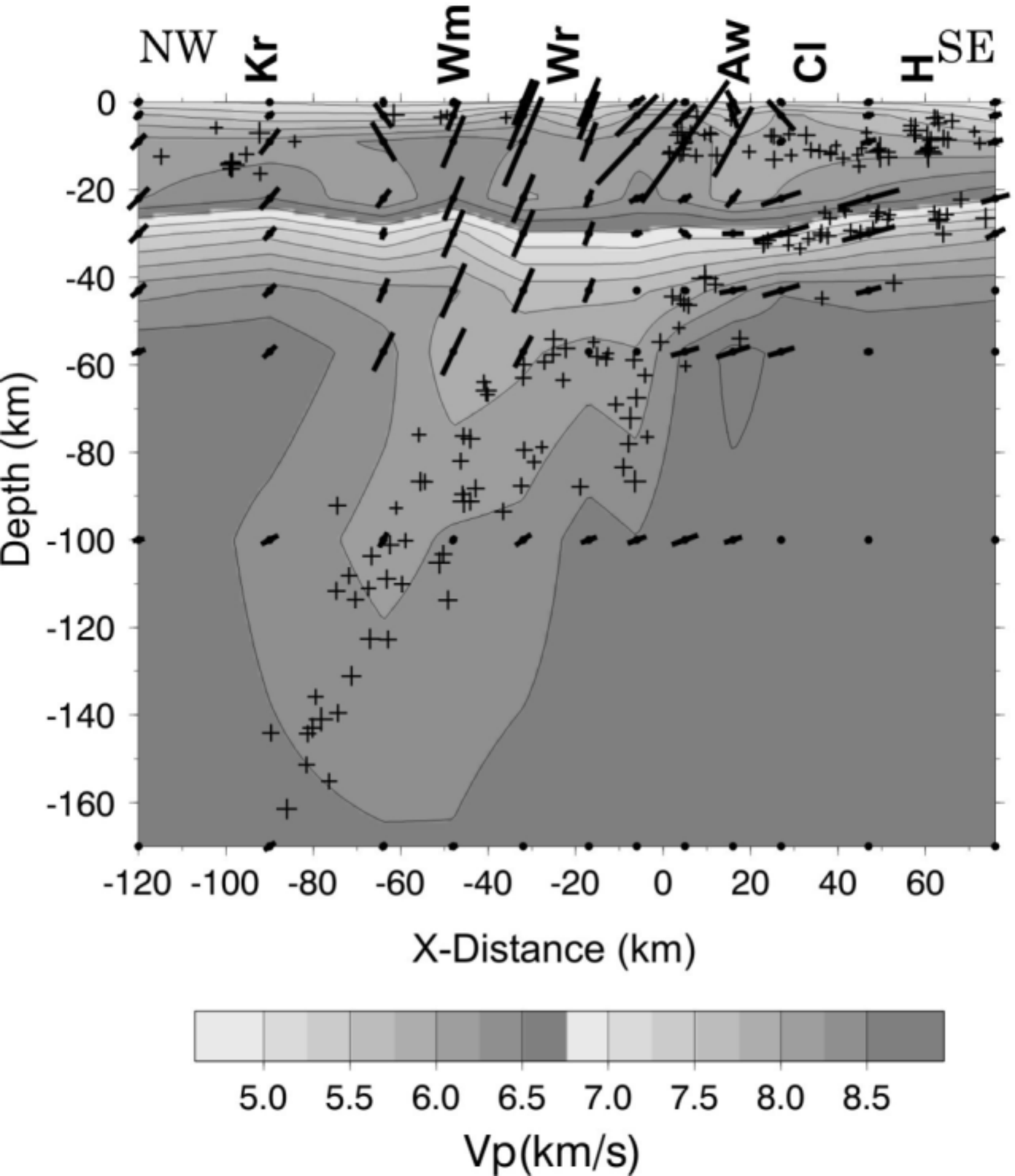
NW
Kr
Wm
Wr
Aw
Cl
H
SE
0
-20
-40
-60
-80
-100
-120
-140
-160
Depth (km)
-120
-100
-80
-60
-40
-20
0
20
40
60
X-Distance (km)
5.0
5.5
6.0
6.5
7.0
7.5
8.0
8.5
Vp(km/s)

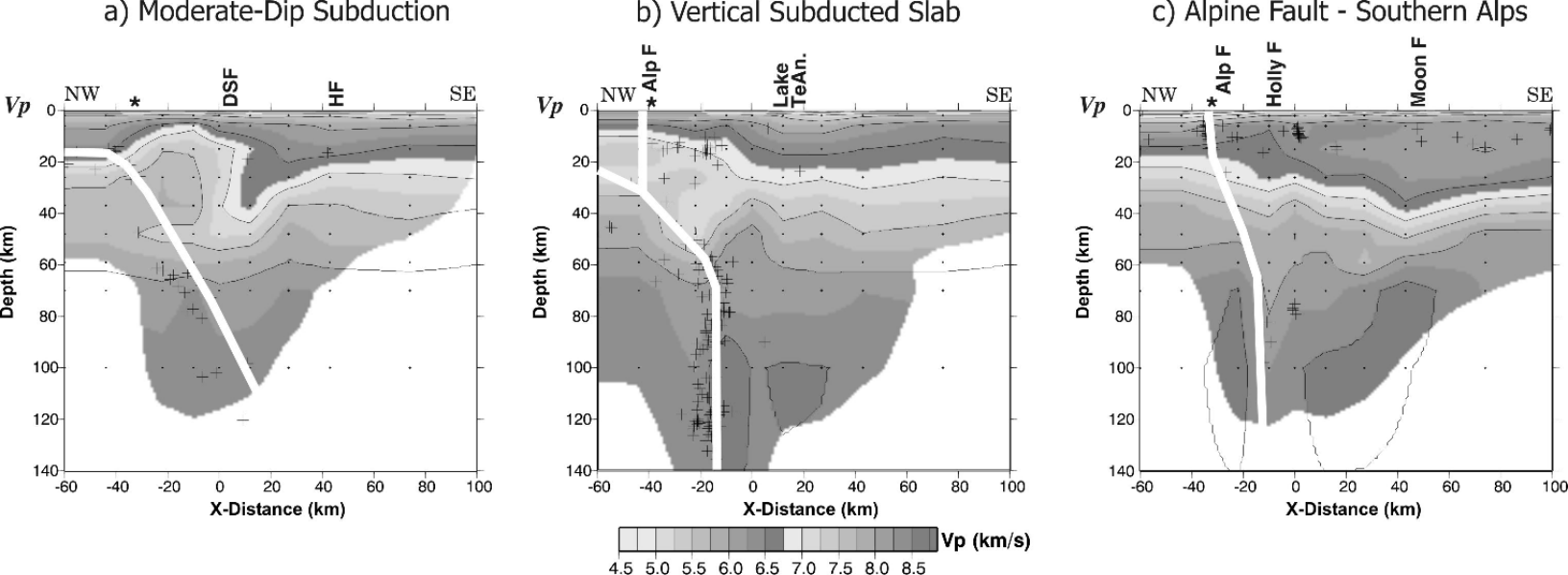
a) Moderate-Dip Subduction
b) Vertical Subducted Slab
c) Alpine Fault - Southern Alps
Vp
NW
SE
DSF
HF
Alp F
Lake TeAn.
Holly F
Moon F
Depth (km)
X-Distance (km)
Vp (km/s)
4.5 5.0 5.5 6.0 6.5 7.0 7.5 8.0 8.5

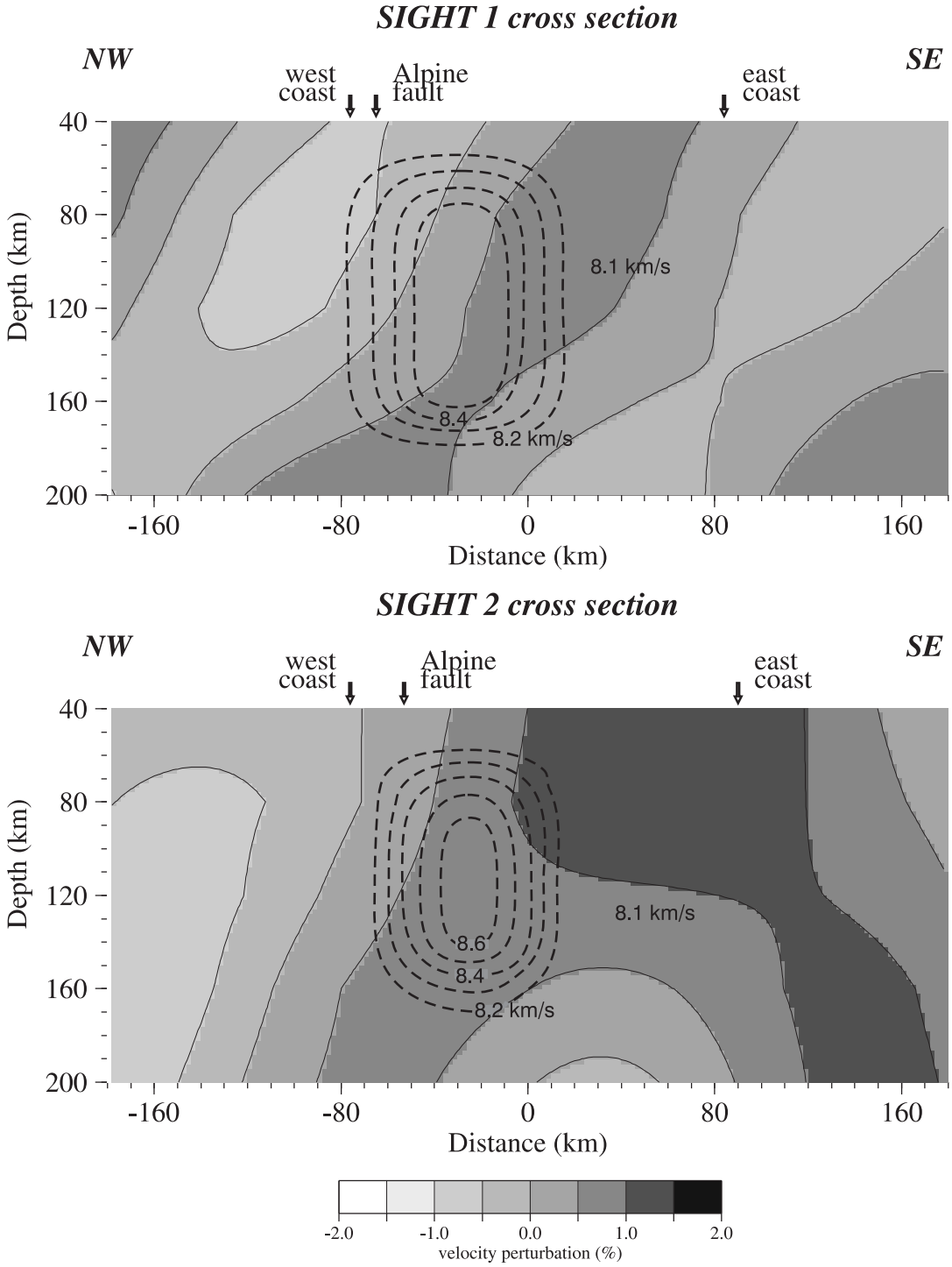
SIGHT 1 cross section
NW
SE
west coast
Alpine fault
east coast
Depth (km)
40
80
120
160
200
-160
-80
0
80
160
Distance (km)
8.1 km/s
8.4
8.2 km/s
SIGHT 2 cross section
NW
SE
west coast
Alpine fault
east coast
Depth (km)
40
80
120
160
200
-160
-80
0
80
160
Distance (km)
8.1 km/s
8.6
8.4
8.2 km/s
-2.0
-1.0
0.0
1.0
2.0
velocity perturbation (%)

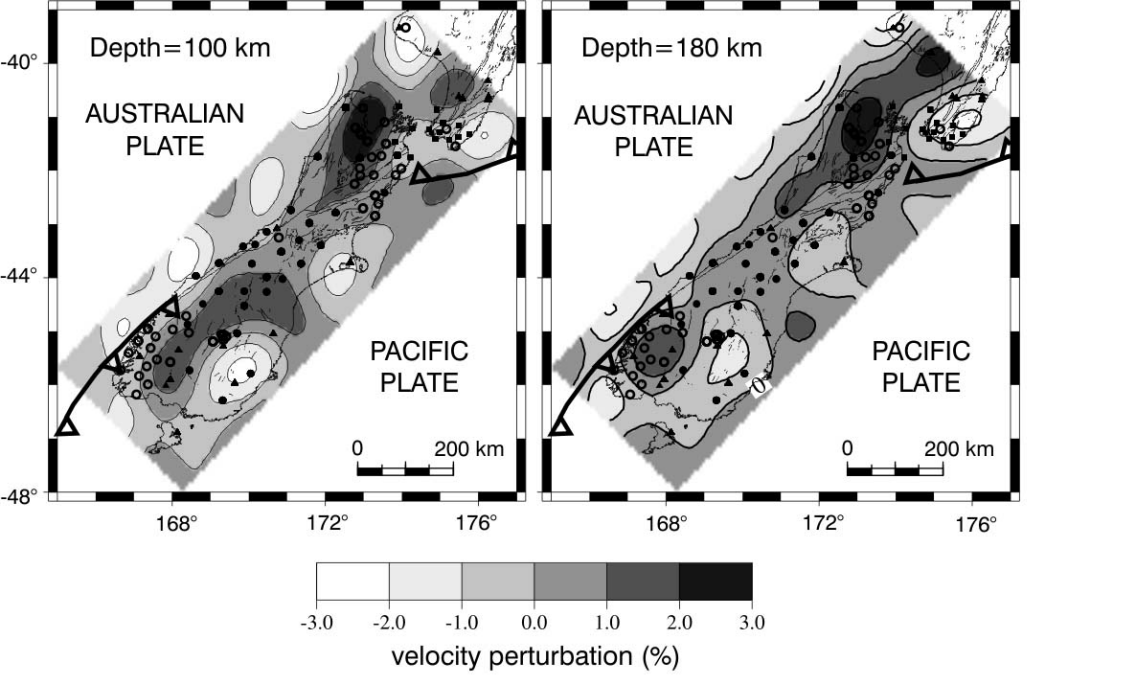
Depth=100 km
AUSTRALIAN PLATE
PACIFIC PLATE
0 200 km
Depth=180 km
AUSTRALIAN PLATE
PACIFIC PLATE
0 200 km
-40°
-44°
-48°
168°
172°
176°
-3.0 -2.0 -1.0 0.0 1.0 2.0 3.0
velocity perturbation (%)

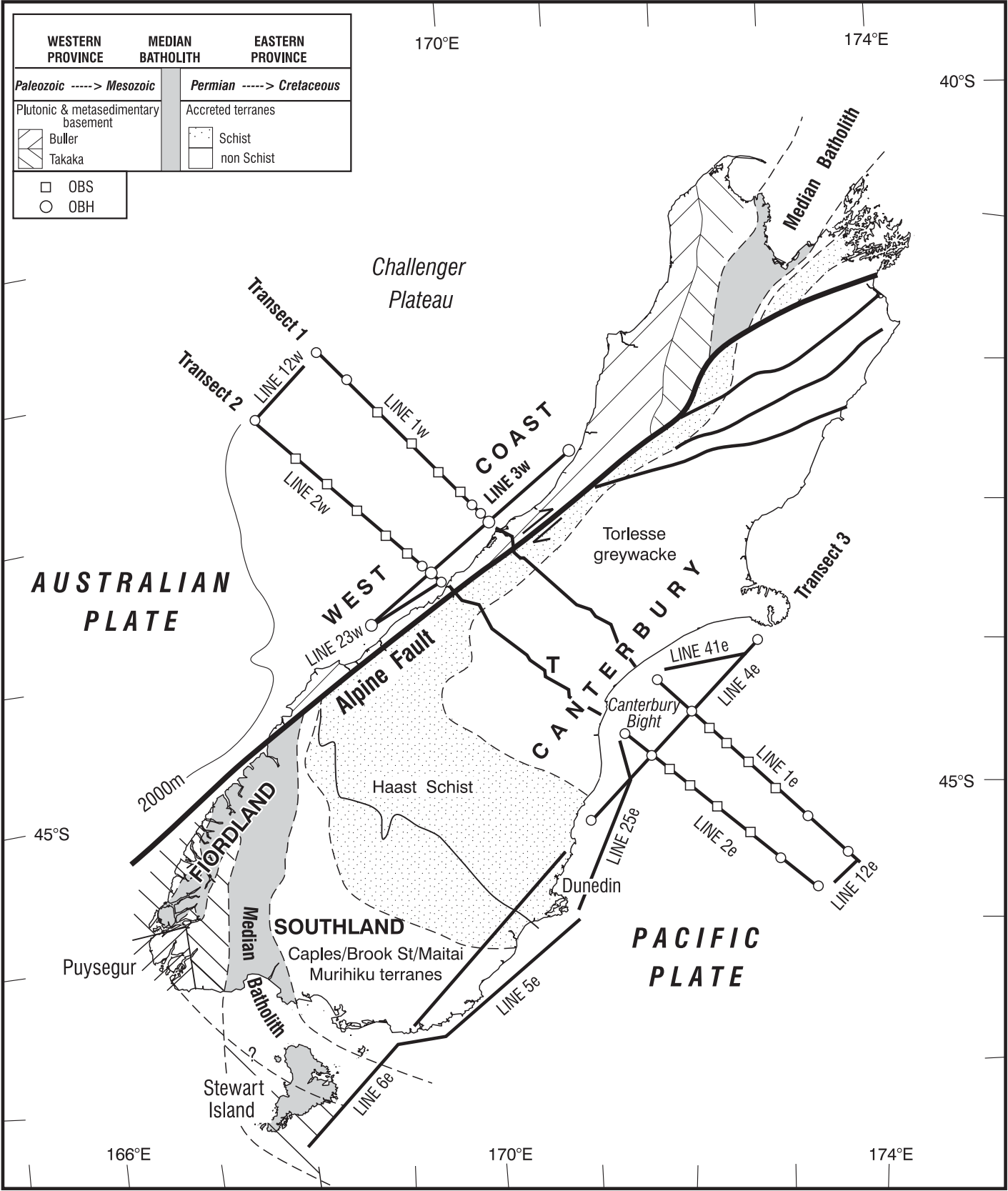
WESTERN PROVINCE
MEDIAN BATHOLITH
EASTERN PROVINCE
Paleozoic -----> Mesozoic
Permian -----> Cretaceous
Plutonic & metasedimentary basement
Buller
Takaka
Accreted terranes
Schist
non Schist
OBS
OBH
170°E
174°E
40°S
45°S
166°E
Median Batholith
Challenger Plateau
Transect 1
Transect 2
LINE 12w
LINE 1w
LINE 2w
LINE 3w
COAST
AUSTRALIAN PLATE
WEST
LINE 23w
Alpine Fault
Torlesse greywacke
Transect 3
CANTERBURY
LINE 41e
LINE 4e
Canterbury Bight
LINE 1e
LINE 2e
LINE 12e
LINE 25e
2000m
Haast Schist
FIORDLAND
Median Batholith
SOUTHLAND
Caples/Brook St/Maitai Murihiku terranes
Puysegur
Dunedin
PACIFIC PLATE
LINE 5e
LINE 6e
Stewart Island

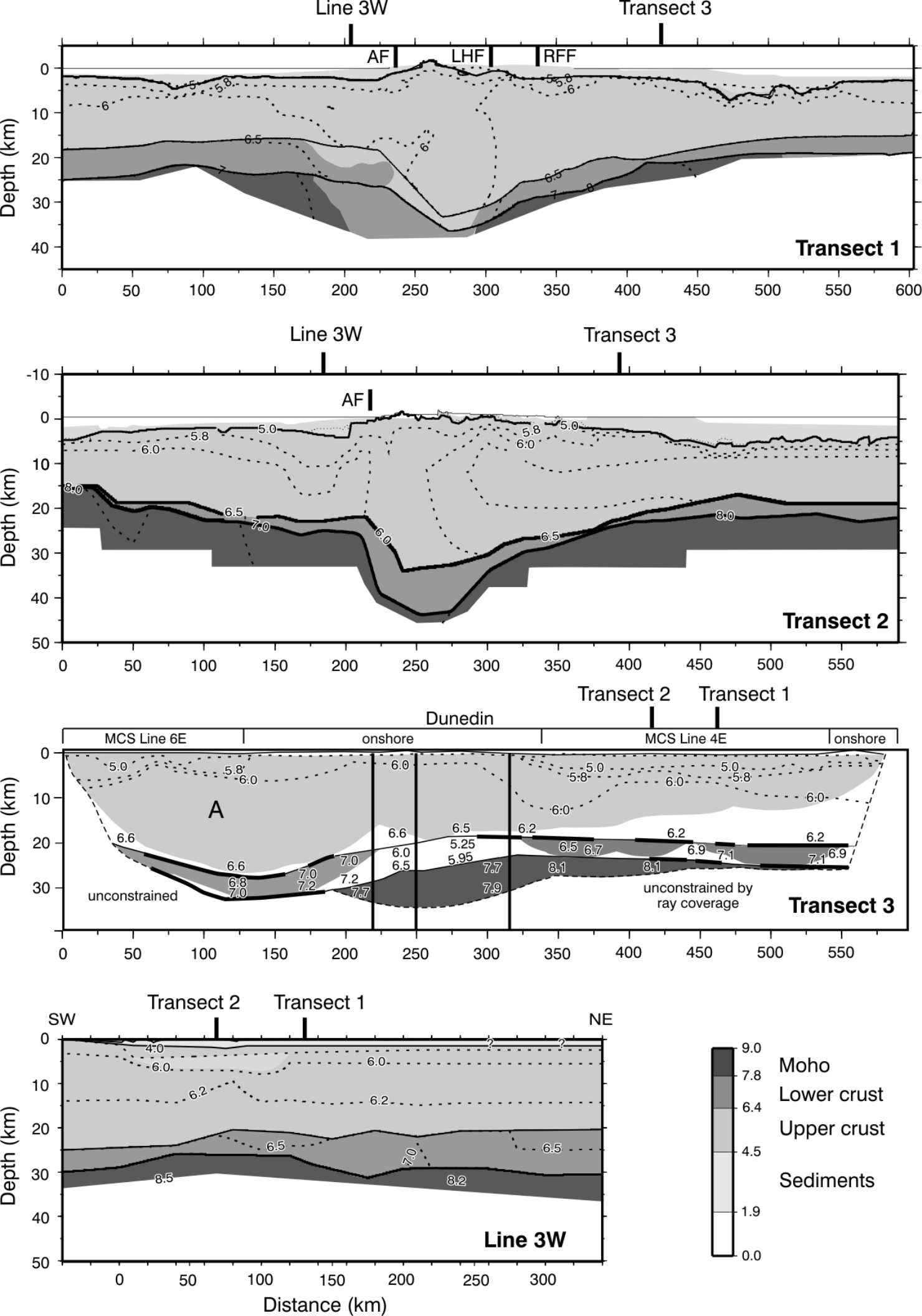
Line 3W
Transect 3
AF
LHF
RFF
Depth (km)
Transect 1
Line 3W
Transect 3
AF
Depth (km)
Transect 2
Transect 2
Transect 1
Dunedin
MCS Line 6E
onshore
MCS Line 4E
onshore
A
unconstrained
unconstrained by ray coverage
Depth (km)
Transect 3
SW
Transect 2
Transect 1
NE
Depth (km)
Line 3W
Distance (km)
Moho
Lower crust
Upper crust
Sediments

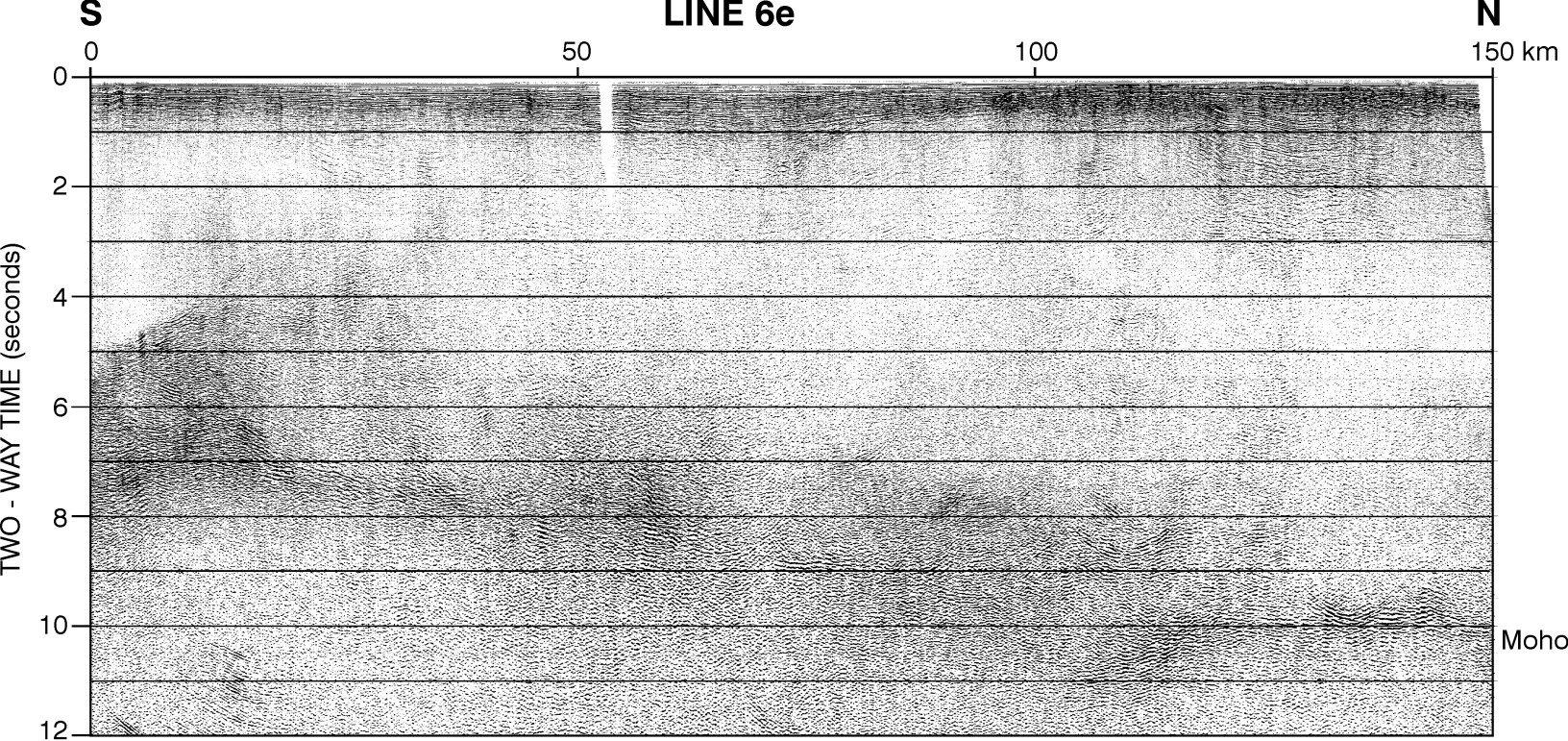
S
LINE 6e
N
0
50
100
150 km
0
2
4
6
8
10
12
TWO - WAY TIME (seconds)
Moho

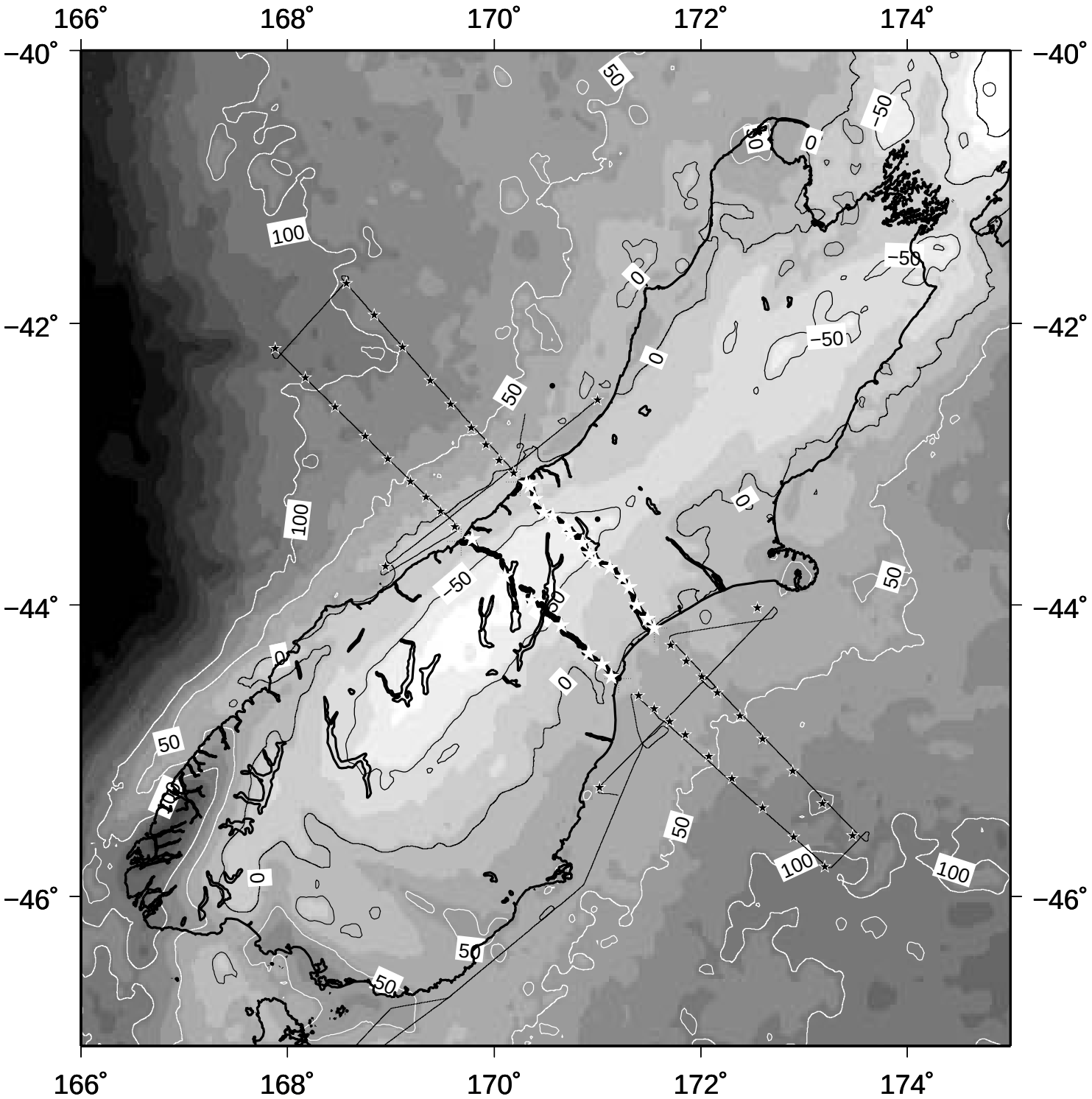
166°
168°
170°
172°
174°
−40°
−42°
−44°
−46°
100
50
0
−50

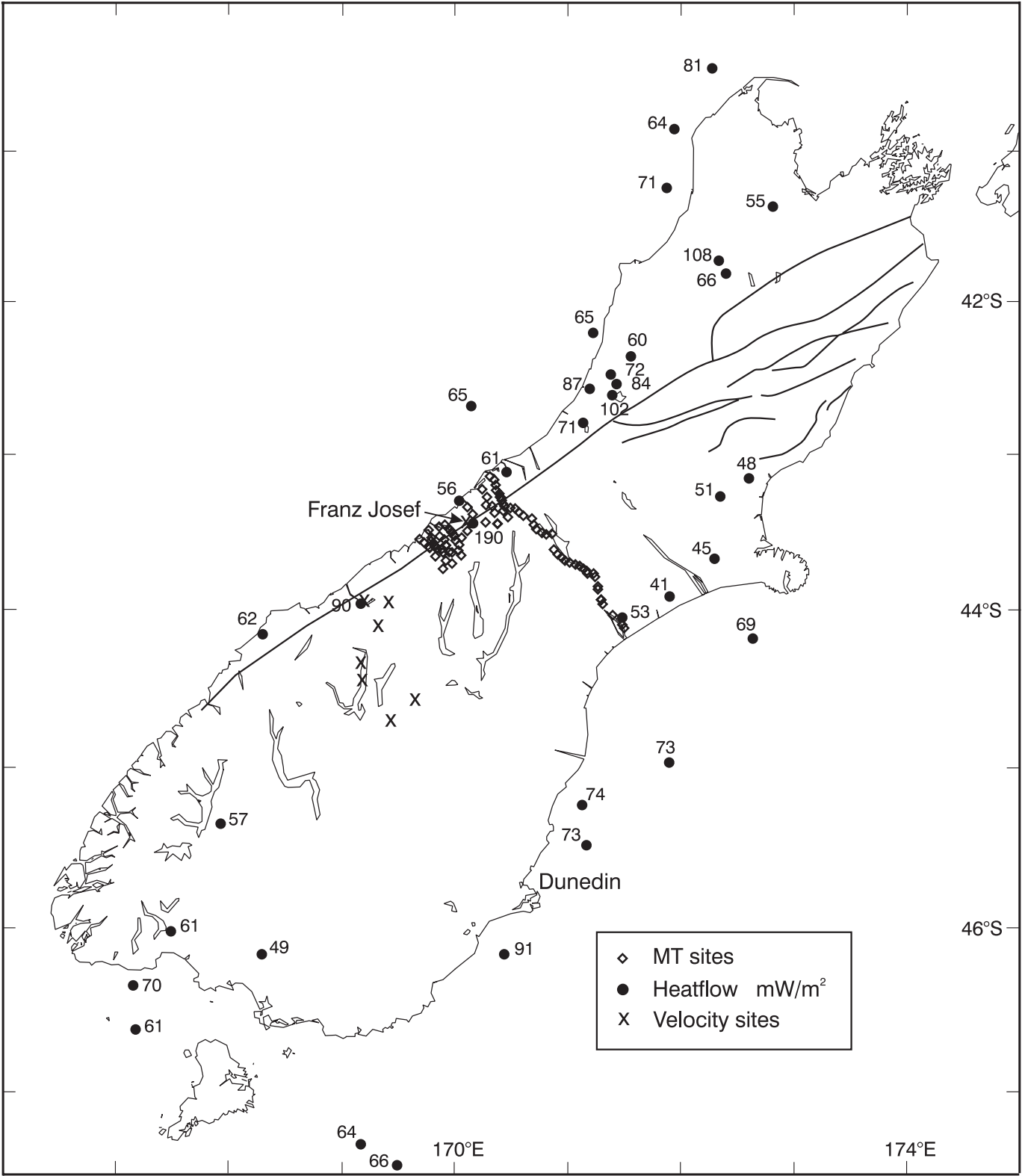
81
64
71
55
108
66
42°S
65
60
72
87
84
102
65
71
61
48
56
51
Franz Josef
190
45
41
62
90
53
44°S
69
73
74
57
73
Dunedin
61
49
91
46°S
70
61
64
66
170°E
174°E
MT sites
Heatflow mW/m²
Velocity sites

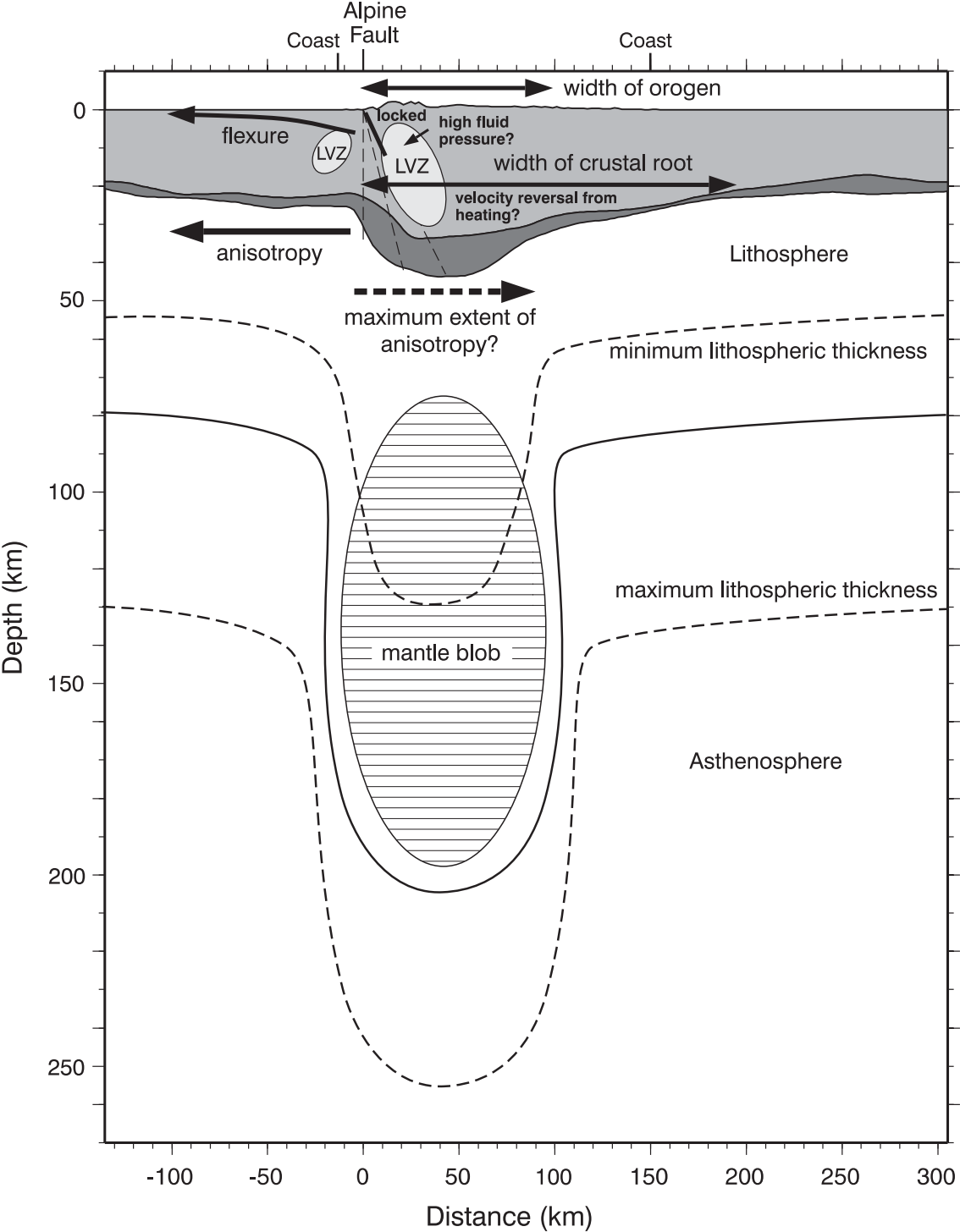
Alpine Fault
Coast
Coast
width of orogen
locked
high fluid pressure?
flexure
LVZ
LVZ
width of crustal root
velocity reversal from heating?
anisotropy
Lithosphere
maximum extent of anisotropy?
minimum lithospheric thickness
maximum lithospheric thickness
mantle blob
Asthenosphere
Depth (km)
0
50
100
150
200
250
-100
-50
0
50
100
150
200
250
300
Distance (km)